ORIGINAL ARTICLE

DOI: https://doi.org/10.18599/grs.2024.1.2 Russian Original 2024. Vol. 26. Is. 1. Pp. 78–99

Identification of the Composition and Assessment of the Influence of the Solid Hydrocarbon Phase in the Reservoir on the Behavior of the Mobile Fluid of the Bazhenov Formation During the Reservoir Development

T.S. Yushchenko[1], I.A. Sannikova[1], M.G. Kulkov[2], A.I. Brusilovsky[1,3], G.T. Salakhidinova[2], A.E. Aliev[2], A.E. Gavrilov[1]*

[1]*Gazprom Neft, St. Petersburg, Russian Federation*
[2]*V.I. Shpilman Research and Analytical Centre for the Rational Use of the Subsoil, Khanty-Mansiysk, Russian Federation*
[3]*Oil and Gas Research Institute of Russian Academy of Sciences, Moscow, Russian Federation*

The purpose of the work is to identify the composition of the initial reservoir hydrocarbon (HC) system of the Bazhenov formation, as well as to assess the influence of the presence of a heavy solid hydrocarbon phase (bitumen) in the formation on the production of mobile fluids using PVT modeling methods. The article describes the necessary experiments to determine the component composition of the C_{81+} fraction and the PVT properties of the formation mobile fluid taken from the well and the bitumen extract from the rock, and also presents their results. In addition, the properties of fractions up to C_{81+} were calculated depending on the molecular weight for PVT modeling (extension of the Katz-Firuzabadi table). One of the important parts of the article is the assessment of the ratio of bound and free oil in the original reservoir system. Based on geochemical research data, an analysis was performed to assess the component composition of the original system (using the example of the Bazhenov Formation) using rock pyrolysis and studying formation fluid and bitumen. Using the results of studies of reservoir fluid samples, a PVT model was built and tuned. This PVT model was used to assess the properties of the initial reservoir hydrocarbon system and was adjusted to the fraction of the solid phase in the reservoir at the initial reservoir conditions. After this, based on the PVT model, an assessment was made of the influence of the presence of a solid phase in the composition of the reservoir system on the behavior of a mobile hydrocarbon fluid during reservoir development for depletion, as well as on the use of enhanced oil recovery methods (injection of associated petroleum gas and thermal methods of influencing the reservoir).

Keywords: Bazhenov formation, PVT model, bitumen, reservoir hydrocarbon system, laboratory studies, geochemical studies

Recommended citation: Yushchenko T.S., Sannikova I.A., Kulkov M.G., Brusilovsky A.I., Salakhidinova G.T., Aliev A.E., Gavrilov A.E. (2024). Identification of the Composition and Assessment of the Influence of the Solid Hydrocarbon Phase in the Reservoir on the Behavior of the Mobile Fluid of the Bazhenov Formation During the Reservoir Development. *Georesursy = Georesources*, 26(1), pp. 78–99. https://doi.org/10.18599/grs.2024.1.2

Introduction

As part of our study to identify the composition of the initial reservoir system of the Bazhenov formation, the heavy hydrocarbon (HC) part, which remains immobile in the reservoir, but is in thermodynamic equilibrium with the mobile fluid, is conventionally called bitumen. In practical terms, by the term "bitumen" in this work we will mean residual petroleum hydrocarbons that can be extracted during the operation of wells using thermal methods of enhanced oil recovery (EOR); they cannot be extracted by hydraulic fracturing methods. Hydrocarbons in the composition of bitumen are represented mainly by resinous-asphaltene components and high-molecular paraffins, located in closed pores or retained by sorption forces on the surface of the kerogen of the Bazhenov formation or by capillary forces in the pores and cracks of the hydraulic fracturing of the Bazhenov formation.

Chloroform extract from rocks of the Bazhenov formation (CBA – chloroform bitumoid, hereinafter referred to as bitumoid) contains hydrocarbons that

---

[*] Corresponding author: Taras S. Yushchenko
e-mail: Yuschenko.TS@gazprom-neft.ru

© 2024 Published by Georesursy LLC
This is an open access article under the Creative Commons Attribution 4.0 License (https://creativecommons.org/licenses/by/4.0/)

can be extracted by hydraulic fracturing (the lightest components) and thermal methods of EOR (mainly the bitumen described above). For 10 samples of extracts of the Bazhenov formation of the studied well, a group and biomarker analysis was carried out, according to the results of which it was established that syngenetic and epigenetic hydrocarbons (bitumoid coefficient β varies from 13 to 50) were generated by organic matter of marine origin, accumulating in marine/lacustrine environments with high content of sulfur (Fig. 1A). The maturity of organic matter (OM) corresponds to the initial stage of the main phase of oil formation (Fig. 1B).

When developing deposits of high-carbon source rocks ("oil shale") in the reservoir, in addition to the moving fluid, bitumen may occur in thermodynamic equilibrium (Muradov et al., 2018). The presence of bitumen will affect the phase behavior and PVT properties of the reservoir fluid during reservoir development, both through depletion and using various enhanced oil recovery (EOR) methods (Cheremisin et al., 2022). The degree of influence will depend on both the amount of bitumen in the formation and its PVT properties. The influence of bitumen on the behavior of formation fluid and its assessment were studied in (Chen et al., 2010; Al Solial et al., 2023). Note that joint accounting of the results of thermodynamic and geochemical studies of reservoir fluids using PVT modeling has not previously been carried out, despite its relevance for the oil and gas industry in connection with the active development of shale oil fields.

To identify the composition and PVT properties of the initial formation hydrocarbon fluid, taking into account bitumen, it is necessary to conduct a series of laboratory thermodynamic, physico-chemical and geochemical studies of samples of formation mobile fluid and rock from one well, because their compositions by area can vary significantly (Ugryumov et al., 2022; Soboleva, 2017; Kozlova et al., 2015). This includes:

- study of the component-fractional hydrocarbon composition up to C_{81+} and thermodynamic studies in a PVT bomb of bottomhole or recombined samples of formation mobile fluid;
- extraction of bitumoid from rock samples, study of the component-fractional hydrocarbon composition up to C_{81+} and general physico-chemical properties of bitumoid;
- pyrolysis of rock samples with an increased number of heating stages. In addition, this includes the construction of a PVT model and its tuning.

Thus, the purpose of this work is to identify the initial composition of the reservoir hydrocarbon system of the Bazhenov formation, taking into account the solid phase, as well as to assess the influence of the solid phase on the behavior of the moving fluid during field development using PVT modeling methods.

The main objectives were:

- development of a methodology for identifying the proportion of bitumen in the composition of the initial reservoir hydrocarbon system based on the analysis of geochemical studies of rock OM and fluids;
- determination of the composition of the initial formation hydrocarbon fluid up to C_{81+}, taking into account bitumen and calculation of the properties of all fractions;
- creation and tuning of a PVT model of the original reservoir hydrocarbon system using the three-parameter cubic Peng–Robinson equation of state (Peng, Robinson, 1976; Péneloux et al., 1982);
- calculation of the influence of the presence of bitumen on the properties of the moving fluid during depletion development and when using EOR for the injection of associated petroleum gas (APG) and thermal effects.

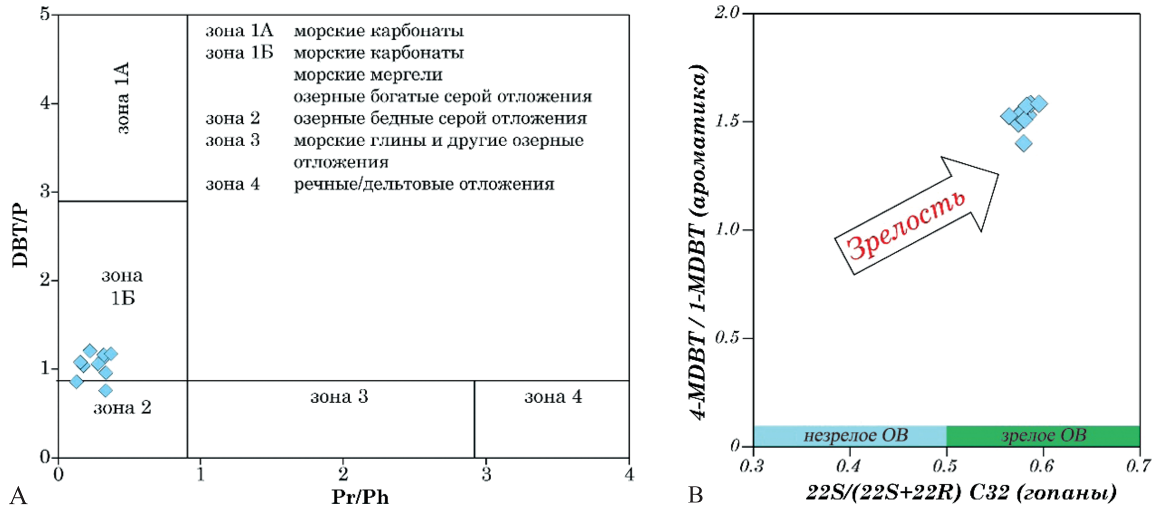

Fig. 1. The ratio of biomarker coefficients characterizing the genesis of hydrocarbons in the Bazhenov formation interval: A – distribution of DBT/PHEN and Pr/Ph coefficients, B – distribution of aromatic and hopane maturity indicators

Analytical studies of organic matter in rock and oil samples

When drilling a pilot borehole, a complete core selection was carried out from the Bazhenov formation interval and pyrolytic studies were performed using the Rock-Eval method with a step of three samples per meter. For this study, a sample of wellhead oil (hereinafter referred to as oil) was taken from the same interval, and two more rock samples were additionally selected (hereinafter referred to as sample No. 1 and sample No. 2) in order to isolate organic extracts (bitumoids) from them. For a sample of oil and extracts isolated from the rock, a complex of studies was carried out – measurement of density and molecular weight, SARA analysis of group composition, as well as determination of the component-fractional composition of hydrocarbons up to C_{81+}.

Rock samples for pyrolytic analysis and extraction were pre-ground to a particle size of less than 500 μm. The oil sample was dehydrated before testing.

Pyrolytic analysis of rock samples

The study was carried out using a HAWK Resource Workstation pyrolyzer (Wildcat Technologies, USA), while for rock samples before extraction, a programmable heating method with an increased number of temperature steps PAM (Petroleum Assessment Method (Maende et al., 2017)) was used: I) heating from 50 °C to 100 °C (5 min isotherm); II) isotherm at 100 °C 5 min; III) heating from 100 °C to 180 °C (5 min isotherm); IV) heating from 180 °C to 350 °C (5 min isotherm); V) heating from 350 °C to 650 °C (5 min isotherm), during which, according to the data of the method developer, sequential thermal desorption of hydrocarbon groups C_4–C_5 (Oil-1 parameter), C_6–C_{10} (Oil-2 parameter), C_{11}–C_{19} (Oil-3 parameter), C_{20}–C_{36} (Oil-4 parameter) occurs, and at the last stage the formation of hydrocarbon products of kerogen cracking and higher molecular weight C_{37+} components (K-1 parameter). In the classical BULK method, when implementing a temperature program of only three steps, it is believed that the main contribution to the intensity of the S_2 peak and its temperature at the maximum is made by the products of kerogen pyrolysis, but for oil shale there can also be a significant proportion of heavy hydrocarbons and resinous-asphaltene components having pyrolytic characteristics close to kerogen (Kalmykov, 2016). Therefore, the increase in the number of temperature steps to 5, proposed by the developers of the PAM method, especially in the area of desorption and cracking of high-molecular compounds, makes it possible to achieve a clearer separation of newly formed hydrocarbons from kerogen cracking products (Maende et al., 2017; Beti, Ring, 2019).

For samples after extraction, additional pyrolytic analysis was performed in BULK mode to control the completeness of bitumoid extraction, as well as to estimate the amount of the heaviest part of bitumoid for further determination of the composition of the reservoir mixture.

According to the pyrolysis data of samples after extraction for a sample covering the entire section of the Bazhenov formation in the studied well, the content of total organic carbon (TOC parameter) and the value of the residual generation potential (HI parameter, or hydrogen index) vary in wide ranges from 1.5% to 19.7% (average 8.6%) and from 277 to 915 mg HC/g TOC (average 629 mg HC/g TOC). The temperature at which the concentration maximum of kerogen pyrolysis products (T_{max} parameter) is recorded varies within the range of 433–446 °C (average value 438 °C).

When characterizing the OM of the rocks of the studied sample by the hydrogen index using the traditional boundaries for distinguishing OM of types I and II (more than 600 and 300–600 mg HC/g TOC, respectively) (Peters, Cassa, 1994), it was found that only a third of the samples belong to type II, and the rest are characterized by increased HI values (from 601 to 915 with an average of 691 mg HC/g TOC), which, at first glance, is not entirely typical for Bazhenov formation rocks (Fig. 2A) (Kontorovich et al., 1998; Lopatin, Yemets, 1999). At the same time, there are works (Samoilenko, 2011; Volkov et al., 2016), in which, based on the analysis of a large array of pyrolytic and mineralogical studies of core material, it is shown that the OM of the Bazhenov formation can also be represented by types I and I–II with characteristic high HI values, as for most of the sample samples considered in this work. In addition, processing of pyrolytic data showed that the samples of the main part of the sample (HI > 600 mg HC/g TOC) are significantly enriched in OM – the average TOC value is 10.6 wt. % versus 4.6 wt. % in samples with HI up to 600 mg HC/g TOC. A similar differentiation of samples can also be traced by the average values of the oxygen index (OI parameter), which, along with the hydrogen index, characterizes the facial-genetic type of OM – in the main part of the sample, the parameter values are significantly lower (2.4 mg CO_2/g TOC) compared to 7.1 mg CO_2/g TOC for the remainder of the samples. An exact determination of the type of OM for samples with elevated HI values in the well under consideration was not carried out due to the lack of necessary additional information and was not the scope of this study.

In general, for the studied section, the increased average value of the residual generation potential with a low average value of the T_{max} parameter indicates a low degree of transformation of rock OM and, as a consequence, an increased content of resinous-asphaltene substances in the formation; accordingly, these rocks will be the most promising for the use of

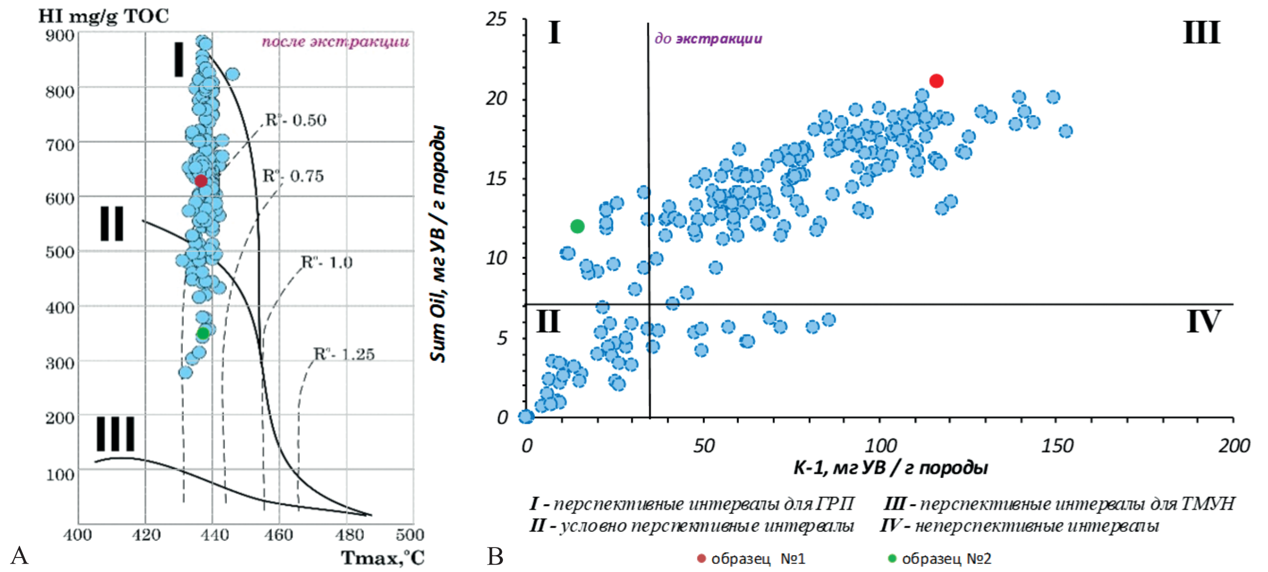

Fig. 2. Modified Van Krevelen diagram (A) and types of promising intervals for the studied samples of the Bazhenov formation (B)

thermal methods of EOR, then for hydraulic fracturing (Fig. 2B) (Spasennykh et al., 2021).

Detailed results of pyrolysis for rock samples No. 1 and No. 2 are presented in Table 1 and are highlighted in the general sample for the studied section in Fig. 2, from which it can be seen that the first of them is representative of the main group of samples with elevated HI values, the OM of which is represented by types I and I–II, and the second sample corresponds to a smaller part of the sample with type II OM. The difference between these samples in the ratio of hydrocarbon groups thermally desorbed up to 350 °C (SumOil parameter) and the products of thermal cracking of kerogen when heated at a stage of 350–600 °C (K-1 parameter) is also significant.

Параметр	Sample 1	Sample 2
Before extraction		
Oil-1, mg/g	0.03	0.19
Oil-2, mg/g	0.44	1.04
Oil-3, mg/g	4.53	4.43
Oil-4, mg/g	10.61	6.33
K-1, mg/g	99.48	14.46
T_{max}, °C	438	440
SumOil, mg/g	15.61	11.99
TOC, wt. %	12.44	4.09
After extraction		
S_0, mg/g	0.13	0.02
S_1, mg/g	0.37	0.11
S_2, mg/g	81.67	8.98
T_{max}, °C	437	438
HI, mg HC/g TOC	625	348
OI, mg CO_2/g TOC	3.00	14.67
GOC, wt. %	7.04	0.82
TOC, wt. %	13.05	2.58
GOC/TOC×100%	53.9	31.7
Estimated bitumoid content based on pre- and post-extraction data (SumOil + (K-1 – S_2))	33,4	17,5

Table 1. Results of pyrolysis and extraction of bitumoids from rock samples. Note: SumOil = Oil-1 + Oil-2 + Oil-3 + Oil-4; GOC – content of pyrolyzable organic carbon in the rock, wt. %; S_0 and S_1 – the amount of thermally desorbed hydrocarbons (thermal evaporation products) at heating stages of 25–150 °C and 150–300 °C, respectively (BULK method); S_2 – amount of hydrocarbon products of kerogen cracking at the heating stage 350–650 °C (BULK method)

Sample No. 1 is significantly enriched in OM, which can be seen from the high values of the SumOil, K-1, and TOC parameters. The T_{max} parameter after extraction for both samples is low (437–438 °C), which, to a first approximation, equally characterizes them as being at the initial stage of the main phase of oil formation, but when assessed using a set of pyrolytic parameters (T_{max} – HI – GOC/TOC×100%), proposed in (Vtorushina et al., 2022; Gutman et al., 2019), the degree of catagenesis of sample No. 1 is determined as PK_3 or MK_1, and of sample No. 2 – MK_2 or $MK_{1–2}$.

Extraction of rock samples

To determine the physico-chemical properties and chromatographic studies of bitumoid, 4–5 g of extract of each sample was isolated from rock samples No. 1 and No. 2. The rock mass required to extract such an amount of bitumoid was determined on the basis of previously obtained data (the ASE accelerated extraction method was used under the conditions given in (Kulkov, Vtorushina, 2019)) on the content of chloroform-soluble bitumoid (CSB) in the samples closest to the section of a given well.

For the purposes of this study, extraction of rock samples was performed in Soxhlet apparatus (extraction head volume 1000 ml) using chloroform as an extractant. Prepared samples were placed in extraction tubes made of filter paper. Extraction was carried out for 138 days for sample No. 1 and 87 days for sample No. 2 with periodic replacement of the solvent with a fresh one. To carry out the planned studies of the extracts and obtain reliable results, taking into account the available instrumentation and methods of its use, it was necessary to free the isolated extracts from the solvent as completely as possible. To do this, the solvent was distilled from the portions of extracts obtained when changing the solvents using a Heidolph rotary vacuum evaporator (Heidolph Instruments GmbH & Co. KG, Germany), the extracts of the corresponding samples were combined, and the CSB content in the rock was calculated from the final mass.

The completeness of the extraction of CSB was determined according to the following criteria (Kontorovich et al., 2018; Tikhonova et al., 2019): no change in the luminescence intensity of the solution (in UV light) in the extraction nozzle of the apparatus after settling overnight; the concentration of the extract in the last two portions of the solution is less than 0.001 wt. %; for extracted rock samples, the sum of parameters $S_0 + S_1 \leq 0.5$ mg/g rock. The OM extracts isolated from samples No. 1 and No. 2 will be designated as bitumoid No. 1 and bitumoid No. 2.

The parameters for the extraction and the results obtained are presented in Table 2.

It is known that when extracts are evaporated using vacuum evaporators, a partial loss of hydrocarbons occurs to C_{18}–C_{19} (Abrams et al., 2017), i.e. gasoline and kerosene fractions, which, in turn, correspond to the sum of the pyrolytic parameters Oil-1, Oil-2 and Oil-3 (Maende et al., 2017). Taking into account the share of these groups from the total amount of thermally desorbed hydrocarbons and resinous-asphaltene components released from the rock during pyrolysis (SumOil + (K-1 – S_2)), the maximum possible losses could be 15.0% for sample No. 1 and 32.4 % for sample No. 2. However, as will be shown below, in the component composition of the isolated CSB, hydrocarbons from C_{15} and above were recorded by the gas chromatographic (GC) method, some of which up to C_{19} inclusive belong to the components of the Oil-3 parameter. Since the sum of components up to C_{19}, according to the GC results, was 6.12 wt. % for sample No. 1 and 17.02 wt. % for sample No. 2, based on the difference between these values and the maximum possible losses, the actual losses for samples No. 1 and No. 2 are estimated at 8.8% and 15.4%, respectively.

According to the extraction data, the bitumoid content (taking into account losses) turned out to be quite close (the difference is no more than 10%) to the estimated bitumoid content based on pyrolytic parameters before and after extraction (parameter SumOil + (K-1 – S_2) in Table 1).

The value of the bitumoid coefficient, calculated from pyrolysis and extraction data (taking into account losses), according to the classification of V.A. Uspensky (Uspensky et al., 1966; Handbook of Geology of Oil and Gas, 1984), characterizes both bitumoids as parautochthonous (having experienced movement within the source rock), at the same time, the values differ significantly, which probably reflects the presence in the sample No. 2 a greater proportion of migratory components, in particular the oil fraction, and, therefore, the possibility of greater movement of bitumoid from the place of generation.

In the section “Restoration of components of the original reservoir system”, the noted losses are taken into account along with the losses of the lightest components when lifting the core from the well, storing and preparing for laboratory tests.

Analysis of physico-chemical parameters (PCP), group and component-fractional composition of bitumoids

Definition of PCP. Molecular mass was determined by cryoscopy in benzene on a KRION-1 apparatus (Termex, Russia) according to the TKLSh 2.843.002 RI[1] method.

Due to their high viscosity at 20 °C, the density of the obtained bitumen was measured for their solutions in toluene, followed by recalculation to the initial state. Solutions were prepared with precise mass concentrations of bitumoid and solvent. Next, their density was measured with an automatic density meter DMA 4500M (Anton Paar, Austria). Taking into account the assumption of the additivity of the densities of the

Parameters	Sample 1	Sample 2
Actual mass of rock taken for extraction, g	145.3	323.6
Actual mass of extract, mg	4032.9	4400.6
Actual CBS content, mg/g of rock	27.8	13.6
Actual CBS content + actual losses, mg/g of rock	30.2	15.7
Bitumoid coefficient (β) taking into account actual losses, %	24.3	38.4

Table 2. Parameters for extraction and results of CSB isolation. Note: CSB – content of chloroform bitumoid in the rock, mg/g of rock; β = (CSB ×0.1/TOC)×100%, where the CSB value in mg/g is converted to % by a conversion factor of 0.1, and the TOC value in % is used from rock pyrolysis data before extraction using the PAM method (Table 1)

---

[1] https://cdn.termexlab.ru/files/c9a56e94/50bd/4281/8d68/b35f5373ac09.pdf

individual components of the mixture (solution), the density of bitumoids was found using the following formula:

$$\rho_{sample} = \frac{(\rho_{solution} - (\rho_{toluene} \cdot m_{toluene} \cdot 0{,}01)) \cdot 100}{m_{sample}} \tag{1}$$

where ρ_{sample}, $\rho_{toluene}$ and m_{sample}, $m_{toluene}$ are the density (g/cm^3) and mass fraction (wt.%) of toluene and sample, respectively.

Determination of group composition (SARA analysis). Asphaltenes were isolated by precipitation in a 40-fold excess of n-hexane, followed by standing in a hermetically sealed flask for 24 hours at room temperature without access to light. The residue after deasphalting (maltenes) was fractionated into three separate groups (saturated hydrocarbons, aromatic compounds, resins) using liquid adsorption column chromatography on silica gel by sequential elution of the groups with solvents of different polarities (Salakhidinova et al., 2022). The elution boundaries of the groups were determined under UV light (λ 365 nm).

Determination of the component-fractional composition of hydrocarbons C_{10}–C_{80} and the unevaporated residue C_{81+}. The analysis was performed using gas chromatography with flame ionization detection. We used the technique of high-temperature simulated distillation (HT SimDis) at reduced pressure (in a flow of inert gas – helium) according to the recommendations of ASTM D7169[2] and ASTM D6352[3] using the equipment complex "Crystal 5000.2" (ZAO SKB "Chromatek", Russia). Based on this analysis, it is possible to obtain indicators of the mass yield of hydrocarbon fractions C_{10}–C_{80} at the boiling point range of 174–675 °C and the unevaporated residue C_{81+}.

The research results obtained in mass fractions were additionally recalculated into mole fractions using the correlation of the molecular weights of petroleum fractions and their boiling points proposed in (Gomaa, El-Hosboudy, 2019), as follows:

1) calculated the amount of substance of each hydrocarbon component and fraction in the composition of oil and bitumoid $\nu_{i(C1–C80)}$, as well as the amount of substance of the oil itself and bitumoid $\nu_{н}$

$$\nu_{i(C1-C80)} = \frac{\omega_{i(C1-C80)}}{Mr_{i(C1-C80)}},\ \nu_{н} = \frac{100}{Mr_o}, \tag{2}$$

where $\omega_{i(C1–C80)}$ and $Mr_{i(C1–C80)}$ are, respectively, the mass fractions (wt. %) and molar masses (g/mol) of the *i*-th hydrocarbon components or fractions of oil and bitumoid up to C_{80}; Mr_o – molar mass of separated oil, g/mol;

2) calculated the amount of substance ν_{C81+} of the unevaporated residue C_{81+} from the difference in the amount of substance of oil and the sum of the amounts of substance of hydrocarbon components and fractions up to C_{80}

$$\nu_{C81+} = \nu_o - \sum \nu_{i(C1-C80)}. \tag{3}$$

3) calculated the content of mole fractions of hydrocarbon components $\varphi_{i(C1–C81+)}$ and fractions up to and including C_{81+} by normalizing the amount of substance of each component to the amount of substance of oil or bitumoid

$$\varphi_{i(C1-C81+)} = \frac{\nu_{i(C1-C81+)}}{\nu_o} \cdot 100\%\ ; \tag{4}$$

4) calculated the molar mass Mr_{C81+} of the unevaporated residue C_{81+}

$$Mr_{C81+} = \frac{\omega_{C81+} \cdot Mr_o}{\varphi_{C81+}}, \tag{5}$$

where ω_{C81+} is the mass fraction of unevaporated residue, wt. %.

The results of the studies (Table 3) showed that bitumen No. 1 is characterized by higher values of density and molecular weight, which is due to a significantly higher proportion of asphaltenes in its composition and a lower content of the saturated hydrocarbon fraction according to SARA analysis. At the same time, bitumoids No. 1 and No. 2 are similar in the content of resins and aromatic compounds. It is also known that data on the group composition of bitumoids can be useful for characterizing their mobility in reservoir conditions based on the ratio of the proportions of more migratory saturated and aromatic groups and less mobile resinous-asphaltene substances (Abrams et al., 2017) and, in relation to the studied samples (Table 3, SAC/RAS parameter), it is clear that the bitumoid from the rock of sample No. 1 is less mobile, which is consistent with the lower value of its bitumoid coefficient (β), and vice versa, the bitumoid of sample No. 2 with a higher value of β in the parameter SAC/RAS are more mobile.

The dependences of the mass fraction of fractions on true boiling temperatures differ significantly for bitumoids (Fig. 3) according to the results of simulated distillation. The proximity of the initial boiling temperatures of 266 °C and 281 °C for bitumoids No. 1 and No. 2, respectively, is associated with the technique used for their extraction from rock samples. The composition of bitumoid No. 1 contains almost two times more heavy fuel fraction 500+ °C (65.3 wt.%), which is consistent with the PCP values and the distribution of SARA groups, and in bitumoid No. 2 (65.8 wt. %) accounts for fuel fractions boiling up to 500 °C (Table 3).

---

[2] ASTM D7169-11. Standard Test Method for Boiling Point Distribution of Samples with Residues Such as Crude Oils and Atmospheric and Vacuum Residues by High Temperature Gas Chromatography. https://www.astm.org/d7169-11.html

[3] ASTM D6352-19e1. Standard Test Method for Boiling Range Distribution of Petroleum Distillates in Boiling Range from 174 °C to 700 °C by Gas Chromatography. https://www.astm.org/d6352-19e01.html

Parameter	Bitumoid 1	Bitumoid 2
PCP		
Molar mass (g/mol)	540.9	388.9
Density at 20 °C, g/cm^3	1.0310	0.9275
Group composition		
Saturated HC, wt. %	11.5	36.0
Aromatic compounds, wt. %	25.3	31.1
Resins, wt. %	26.3	24.9
Asphaltenes, wt. %	36.9	8.0
Oils/CAB**	0.6	2.0
Fractional composition		
Gasoline up to 200 °C (HC up to $C_{11–12}$), wt. %	0.0	0.0
Kerosene 200–300 °C (HC $C_{11–12}$ – $C_{17–18}$), wt. %	1.9	6.2
Oil and gas oil 300–500 °C ($C_{17–18}$ – $C_{36–37}$), wt. %	32.8	59.6
Fraction 500+ °C ($C_{36–37+}$), wt. %	65.3	34.2
Boiling point, °C	266	281

Table 3. Physico-chemical properties (PCP), group and fractional composition of bitumoids. Data are presented for stabilized bitumoids (without volatile fractions). ** SAC = saturated hydrocarbons + aromatic compounds; RAS (resinous-asphaltene substances) = resins + asphaltenes

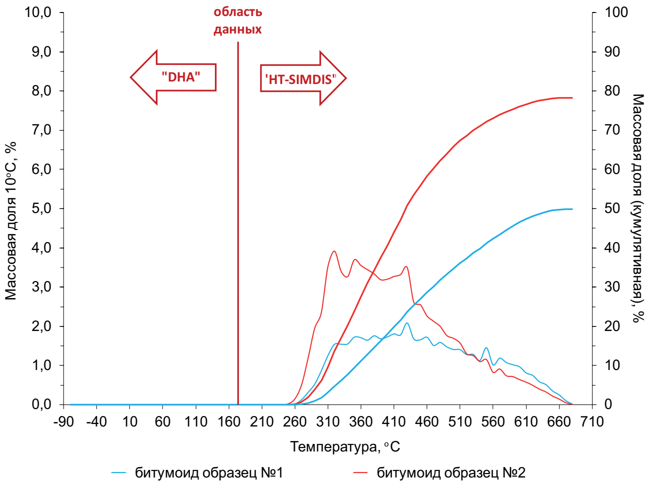

Fig. 3. Diagrams of the concentration distribution of hydrocarbon fractions of bitumoid over 10-degree boiling-off intervals (solid curve – ordinate axis on the left; dotted curve – ordinate axis on the right)

Diagrams of the distribution of hydrocarbon fractions of bitumoid samples No. 1 and No. 2 by mass and mole fractions of molecular weight and number of carbon atoms are shown in Fig. 4, where it is clear that the maximum concentration distribution of hydrocarbons falls on the C_{19}–C_{20} fractions with a molar mass range of 265–279 g/mol. The greatest difference in concentration profiles is observed in the region of hydrocarbon fractions up to C_{33}–C_{37}, which corresponds to components with a molecular weight of up to 430–468 g/mol.

Data on individual C_{n+} fractions, i.e. by fractions with the number of carbon atoms from the specified value *n* and above, in the composition of bitumoid are given in Table 4, from which the most dramatic difference in the concentrations of high-boiling C_{n+} fractions (C_{36+}, C_{81+}) is visible. Bitumoid No. 1 is characterized by a higher molar mass of all C_{n+} fractions.

Analytical studies of oil sample

For an oil sample, the determination of molecular weight, group and component-fractional composition was carried out according to the above methods for studying bitumoid. In addition to gas chromatographic analysis using the HT SimDis method, light hydrocarbons C_1–C_9 were analyzed (Detailed Hydrocarbon Analysis, DHA) according to ASTM D7900[4] and ASTM D6730[5] using a gas chromatograph with a flame ionization detector and a cooling system for the chromatograph thermostat "Crystal 5000.2" (JSC SKB "Chromatek", Russia). The results of oil analysis carried out by the DHA and HT SimDis methods are combined using the Chromatek Distillation software package to obtain the final component-fractional composition of hydrocarbons C_1–C_{80} and the unevaporated residue C_{81+}. *n*-nonane was taken as the boundary component when combining the DHA and HT SimDis data. As for bitumoid, the data obtained in mass fractions were additionally recalculated into mole fractions.

The results of oil sample studies are given in Table 5 and in Fig. 5.

According to laboratory studies, bitumoid No. 1 is characterized by a significantly higher content of the heavy fraction C_{81+}, the main share of which is probably represented by asphaltenes, in contrast to bitumoid No. 2, in which resins predominate in the composition of the dry substances. In addition, most of the SAC fraction of bitumoid No. 1 is formed by aromatic compounds. Higher values of the density and molecular weight of

---

[4] ASTM D7900-17. Standard Test Method for Determination of Light Hydrocarbons in Stabilized Crude Oils by Gas Chromatography. https://www.astm.org/d7900-17.html

[5] ASTM D6730-19. Standard Test Method for Determination of Individual Components in Spark Ignition Engine Fuels by 100-Metre Capillary (with Precolumn) High-Resolution Gas Chromatography. https://www.astm.org/d6730-19.html

Fraction C_{n+}	Bitumoid 1	Bitumoid 2
A weight ratio of the fraction, %		
C_{7+}	100.0	100.0
C_{13+}	100.0	100.0
C_{20+}	93.9	83.0
C_{36+}	67.2	36.1
C_{81+}	50.4	21.8
A mole ratio of the fraction, %		
C_{7+}	100.0	100.0
C_{13+}	100.0	100.0
C_{20+}	86.7	73.1
C_{36+}	45.5	19.8
C_{81+}	28.8	9.3
Molar mass of the fraction, g\mol		
C_{7+}	540.9	389.0
C_{13+}	540.9	389.0
C_{20+}	585.7	441.4
C_{36+}	798.5	708.1
C_{81+}	947.1	909.7

Table 4. Properties of individual C_{n+} fractions of bitumoids

bitumoid No. 1 indicate a large proportion of high-molecular compounds in its material composition; accordingly, rock sample No. 1 contains significantly more bitumen. To assess the influence of the presence of bitumen on the properties and behavior of reservoir mobile oil during reservoir development, bitumoid No. 1 was selected.

Based on data on the calculation of the molecular weight of fractions up to C_{80}, the Katz–Firoozabadi table was expanded (Katz, Firoozabadi, 1978; Whitson, Brulé, 2000) (Appendix B). The density of the fractions was calculated according to the Hassan method (Naji, 2010), the average boiling point was taken according to reference data ASTM D7169. The critical parameters of the fractions were calculated using the method described in (Yushchenko, Brusilovsky, 2022), in which the critical temperature is determined by the Lee – Kesler correlation (Lee, Kesler, 1975), the acentric factor – by the Riazi – Al-Sahhaf correlation (Riazi, Al-Sahhaf, 1996), and the critical pressure using the cubic three-parameter Peng–Robinson equation of state under standard conditions for each fraction.

PVT study of reservoir oil

Reservoir oil was obtained based on wellhead sampling of gas and oil and recombination of the reservoir system according to three GOR values: 23, 53, 125 m³/m³. This was done due to the lack of reliable measurements of the oil-gas ratio (GOR) in the field, as well as to assess the influence of bitumen on the PVT properties and phase behavior of reservoir mobile oil with different contents of dissolved gas during reservoir development.

For recombined samples of reservoir oil from the Bazhenov formation, a standard set of laboratory tests was carried out in a PVT cell: contact composition expansion at reservoir temperature, single flash and the dependence of the dynamic viscosity of reservoir oil on pressure at reservoir temperature. As a result of the studies, the composition of reservoir oil up to C_{81+}, saturation pressure at reservoir temperature, isothermal

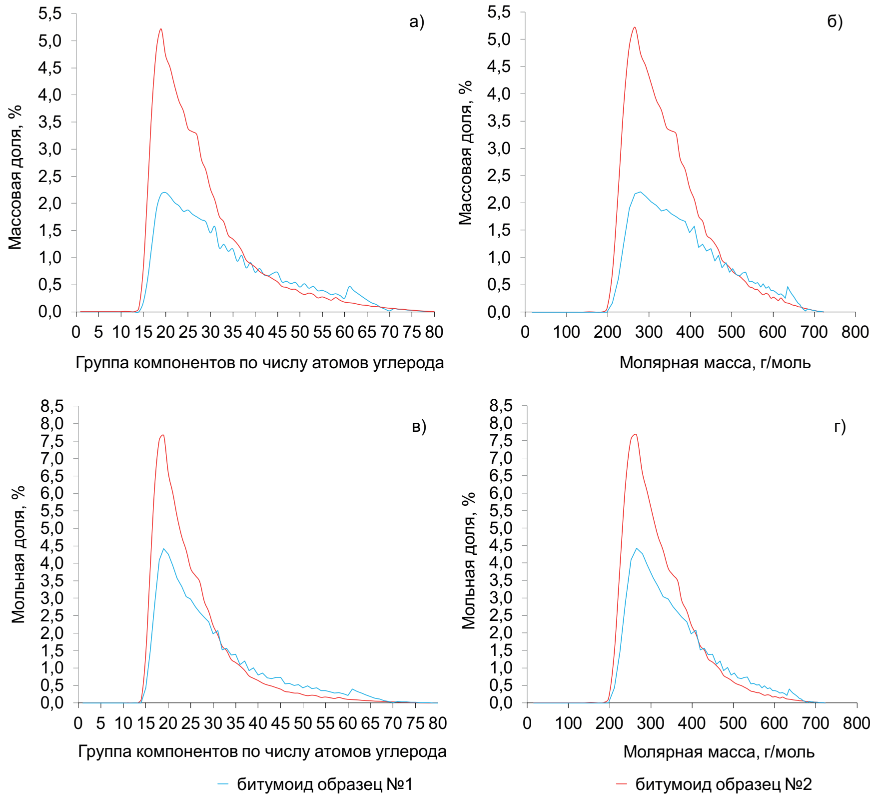

Fig. 4. Diagrams of molecular weight distribution of hydrocarbon fractions up to C_{80}

Parameter			OIL
Physicochemical parameters			
Molar mass, g/mol			234.5
Density at 20 °C, g/cm^3			0.8701
Group composition			
Saturated HC, wt. %			31.6
Aromatic compounds, wt. %			43.1
Resins, wt. %			23.5
Asphaltenes, wt. %			1.9
Oils/CAB			2.9
Fractional composition			
Gasoline up to 200 °C (HC up to $C_{11–12}$), wt. %			21.8
Kerosene 200–300 °C (HC $C_{11–12}$ – $C_{17–18}$), wt. %			16.7
Oil and gas oil 300–500 °C ($C_{17–18}$ – $C_{36–37}$), wt. %			31.7
Fraction 500+ °C ($C_{36–37+}$), wt. %			29.9
Boiling point, °C			-0.5
Properties of individual C_{n+}-fractions			
Fraction	Weight ratio, %	Mole ratio, %	Molar mass, g/mol
C_{7+}	94.5	82.4	269.1
C_{13+}	75.9	48.7	365.2
C_{20+}	55.7	27.1	482.4
C_{36+}	31.2	10.5	695.6
C_{81+}	19.3	5.3	851.1

Table 5. Physico-chemical parameters, group and fractional composition, properties of individual C_{n+} fractions of oil. Note: the group composition is given in terms of the stabilized part of the oil (without volatile fractions)

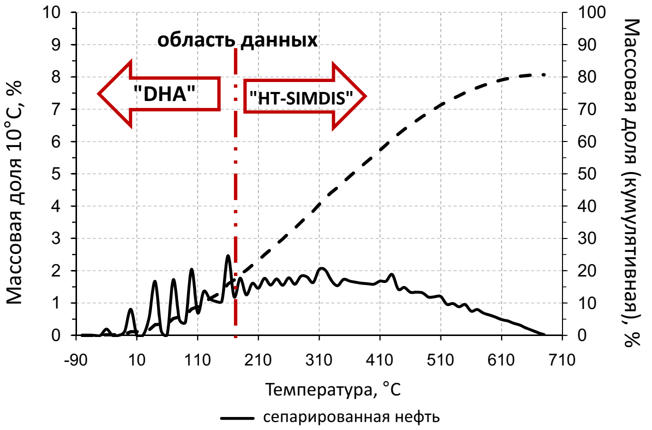

Fig. 5. Diagrams of the concentration distribution of hydrocarbon fractions of oil over 10-degree boiling-off intervals (solid curve – ordinate axis on the left; dotted curve – ordinate axis on the right)

compressibility coefficient from the initial reservoir pressure to saturation pressure at reservoir temperature, and the dependence of the dynamic viscosity of reservoir oil on pressure at reservoir were determined. The results of laboratory tests are presented in Table 6, the composition of separated oil, dissolved gas and reservoir oil is in Appendix A.

Based on data on the composition of reservoir oils up to C_{81+}, a PVT models was created using the cubic three-parameter Peng-Robinson equation of state (Peng, Robinson, 1976; Péneloux et al., 1982) and mathematical algorithms for calculating vapor-liquid equilibrium (Brusilovsky, 2002; Michelsen, Mollerup, 2007). In the PVT model, to increase the speed and quality of calculations, the fractions were grouped into the following pseudo fractions: $C_{6–7}$, $C_{8–9}$, $C_{10–11}$, $C_{12–13}$, $C_{14–16}$, $C_{17–19}$, $C_{20–23}$, $C_{24–27}$, $C_{28–31}$, $C_{32–37}$, $C_{38–42}$, $C_{43–49}$, $C_{50–56}$, $C_{57–63}$, $C_{64–71}$, $C_{72–80}$, C_{81+}. Pure components did not group with each other. The PVT model of reservoir oil was tuned to the results of laboratory studies using a step-by-step adjustment method, described in detail in (Yushchenko, Brusilovsky, 2022). The tuning results are given in Table 6 and in Fig. 6.

Further, these PVT models were used to assess the influence of the presence of bitumen on the phase behavior and PVT properties of reservoir mobile oil in the initial reservoir hydrocarbon system of the Bazhenov formation.

Restoration of components of the original reservoir system

Calculation of the mass ratio of mobile fluid and bitumen in the rock (at initial reservoir conditions) for two studied samples (samples No. 1 and No. 2) was performed based on HAWK-PAM pyrolysis data before extraction and pyrolysis after extraction, as well as using component-group composition of extracts of these samples, degassed and recombined samples of oils up to C_{81+}. Since the component composition of the recombined reservoir oil sample is known, in order to determine the proportion of these mobile components, you need to know the sum of all components in the reservoir (oil + bitumen). This amount can be obtained based on the component composition of bitumoid (CSB), since by extracting the rock powder, we extract both free hydrocarbons and sorbed hydrocarbons, as well as

Parameters	Gas content					
	$23\ m^3/m^3$		$53\ m^3/m^3$		$125\ m^3/m^3$	
	Fact	PVT-model	Fact	PVT-model	Fact	PVT-model
Reservoir pressure P_{res}, bar	295					
Reservoir temperature T_{res}, °C	100					
Saturation pressure, bar	56.8	56.5	109	109	191.8	190.3
Density of reservoir oil at P_{res} and T_{res}, kg/m^3	827	828	821	817	818	818
Viscosity of reservoir oil at P_{res} and T_{res}, cP	4.16	4.19	1.8	1.9	0.7	0.7
Compressibility coefficient of formation oil, $\times 10^{-5}$ 1/bar	10.4	9.9	18.6	18.4	23.7	23.8
Standard separation						
Volume factor of reservoir oil at P_{res} and T_{res}, un.	1.077	1.075	1.128	1.129	1.240	1.242
Gas content, m^3/m^3 (m^3/t)	23.1 (27)	22.4 (27)	53.1	52.2	125	124
Density of separated oil, kg/m^3	863	862	863	862	863	864
Dissolved gas density, kg/m^3 (relative density)	1.23 (1.02)	1.24 (1.03)	1.21 (1.01)	1.22 (1.02)	1.21 (1.01)	1.22 (1.02)

Table 6. Properties of reservoir oils with different gas contents, defined during laboratory studies and PVT modeling

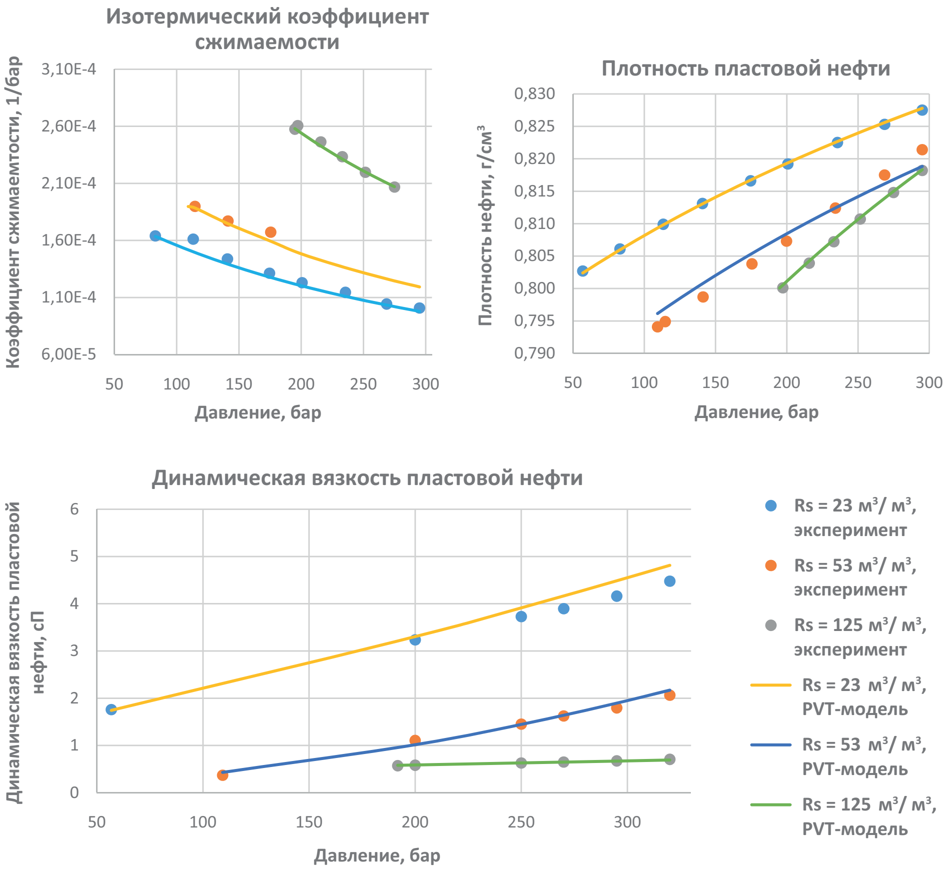

Fig. 6. Dependence of density, viscosity and isothermal compressibility coefficient of reservoir oil on pressure at reservoir temperature

heavy hydrocarbons from the early stages of generation and hydrocarbons from closed pores. However, it is known that when lifting the core, light hydrocarbons evaporate, and we will not find them in the extract, so the conditional equation is valid:

Oil + Bitumen = Bitumoid (CSB) + HC losses.

A schematic distribution of the hydrocarbon composition of the reservoir system is shown in Fig. 7, where the heavy fractions found only in bitumen are highlighted in black. In fact, in the phases of bitumen and oil that are in thermodynamic equilibrium in the reservoir, all hydrocarbons from C_1 to C_{81+} will be found, with the overwhelming share of bitumen being fractions from C_{40+} and heavier, and the predominant part of hydrocarbon losses during evaporation being components up to C_{15+}.

A similar distribution is visible in the histogram of the component composition of reservoir oil for gas hydrocarbons, starting from methane to the C_{81+} component, and in the histogram of the component composition of bitumoid No. 1 for C_{15}–C_{81+}. It can

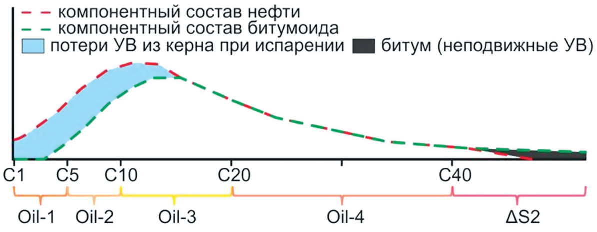

Fig. 7. Schematic distribution of the components of the original reservoir system, incl. oils, bitumen, taking into account pyrolytic peaks

be seen that the studied bitumoid sample most likely completely lost the C_1–C_{14} components during lifting and storage, as well as during sample preparation for pyrolytic analysis (during rock crushing). Components C_{14}–C_{19} were also partially lost during the isolation process (evaporation from the solvent is a technological loss, since analyzes with traces of solvent are unreliable). The noted losses are clearly visible in Fig. 8.

The recovery of HC losses was carried out through the pyrolytic peaks of samples of rocks that had not yet been extracted, since it is known that in peaks Oil-1 on the pyrogram the yields of components C_1–C_5 are recorded, Oil-2 – C_6-C_{10}, Oil-3 – C_{11}–C_{19}, Oil-4 – C_{20}–C_{40}, and the difference between K-1 peaks before and S_2 after extraction (ΔS_2) corresponds to C_{41+} compounds. Having compared the distributions of the components of recombined oil and bitumoid visually (Fig. 6), it can be noted that in the graphs of the distribution of the hydrocarbon part from C_{20} to C_{40} in both oil and bitumoid they have a similar appearance, hence we can conclude that these compounds, throughout visibility have not undergone significant changes due to evaporation. The main losses of hydrocarbons from the rock are associated with components C_1–C_{20} (i.e., with the peaks Oil-1, Oil-2, Oil-3).

By adding the mass fractions of the components of the recombined oil samples (Appendix A), the mass fractions of the components were found for the following groups: C_1–C_5, C_6–C_{10}, C_{11}–C_{19}, C_{20}–C_{40}, C_{41+}. The mass fractions of these groups were taken to be the ratios Oil-1, Oil-2, Oil-3, Oil-4 and Oil 5 in the absence of bitumen and their sum was equal to 100%. Then this amount of group composition was recalculated to 100% only for 4 groups (Oil-1, Oil-2, Oil-3, Oil-4), as a result, group shares of hydrocarbons were obtained without taking into account losses, which for Oil-1 amounted to 8.44 wt. %, for Oil-2 – 20.79 wt. %, for Oil-3 – 35.34 wt. %, for Oil 4–35.43 wt. % for a recombined oil sample with a gas oil ratio of 23 m^3/m^3. Calculation of the Oil-1, Oil-2, Oil-3 values for bitumoid samples was carried out using the formulas

$$\mathrm{Oil}-1\ (\mathit{with\ losses}) = \frac{8.44 \cdot \mathrm{Oil}-4\ (\mathit{without\ losses})}{35.43} \tag{6}$$

$$\mathrm{Oil}-2\ (\mathit{with\ losses}) = \frac{20.79 \cdot \mathrm{Oil}-4\ (\mathit{without\ losses})}{35.43} \tag{7}$$

$$\mathrm{Oil}-2\ (\mathit{with\ losses}) = \frac{20.79 \cdot \mathrm{Oil}-4\ (\mathit{without\ losses})}{35.43} \tag{8}$$

The calculation of the Oil-1, Oil-2, Oil-3 values, taking into account losses, was carried out from the value of the Oil-4 peak, since the components in this group did not experience any loss as if the core sample were sealed. Figure 9 shows graphs of the ratio of peaks Oil-1, Oil-2, Oil-3, Oil-4 based on the results of pyrolytic studies for samples of the Bazhenov formation (blue dots). Separately displayed are the samples used in calculating the proportions of the components of the original reservoir system (dots in red and light green). The marsh-colored dots show the values of the corresponding peaks Oil 1, Oil-2, Oil-3 calculated using formulas (6)–(8) on the graphs, taking into account losses under the accepted assumptions. Arrows on the graphs in Fig. 9 shows the trend of loss recovery.

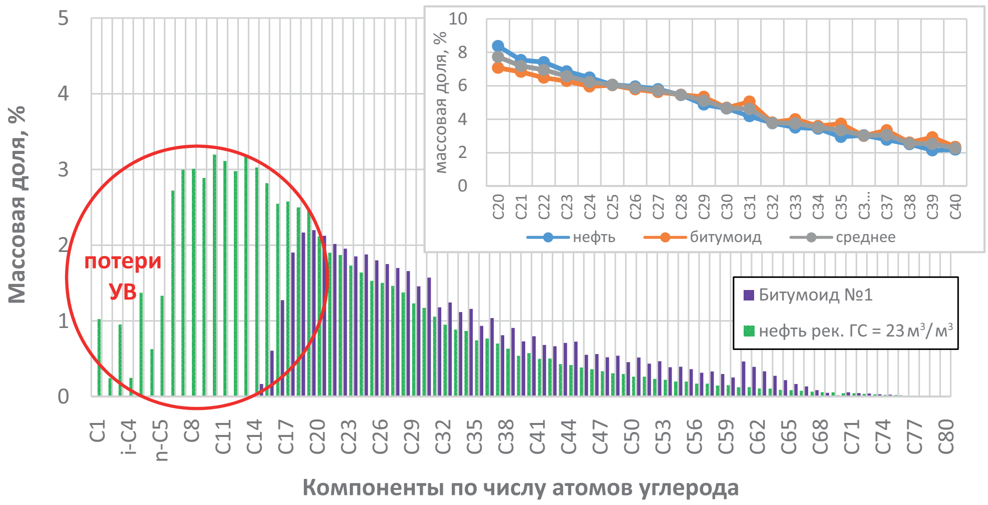

Fig. 8. Comparison of mass fractions of the component composition of bitumoid No. 1 and a recombined oil sample with a solution GOR equal to 23 m^3/m^3

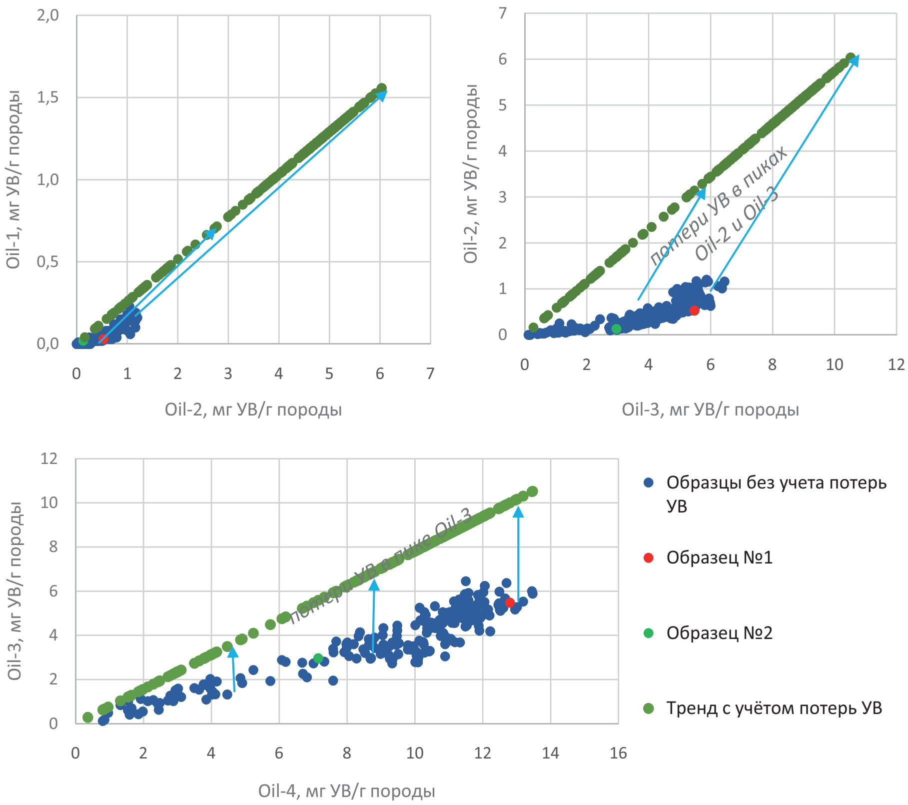

Fig. 9. Trend in recovery of hydrocarbon losses based on recalculation data of pyrolytic parameters

The values of the hydrocarbon potential of rocks and the restored value of bitumoid, taking into account losses in each sample and in each peak, are presented in Table 7. It is worth emphasizing that the Oil-5 value for bitumoid includes both C_{41+} components in oil and C_{41+} components in bitumen (the stationary part of the original reservoir system). To divide the group of Oil-5 components into moving and stationary parts, the dependences of the mass fraction of recombined oil (%) on the value of rock potential (mg HC/g of rock) were plotted for groups Oil-1, Oil-2, Oil-3, Oil-4 according to Table 7. For both samples studied, the dependence was described by linear equations

$$\text{Oil-5 moving part} = 0.4558x - 0.0039,\ \text{mg HC/g rock (sample No. 1)}, \quad (9)$$

$$\text{Oil-5 of the moving part} = 0.2504x - 0.0011,\ \text{mg HC/g rock (sample No. 2)}, \quad (10)$$

where x is the proportion of recombined oil in the Oil-5 group, wt. %.

From relations (9)–(10) the value of Oil-5 (mgHC/g rock) was found in the part of mobile hydrocarbons. The value of Oil-5 components in the bitumen area was determined as the difference between the Oil-5 value in bitumoid and the Oil-5 value in the part of mobile hydrocarbons. Note that for sample No. 2, the value of mobile hydrocarbons in the Oil-5 group exceeds the

Samples	Bitumoid including losses					Bitumoid excluding losses				
	$C_{1–5}$	$C_{6–10}$	$C_{11–19}$	$C_{20–40}$	C_{41+}	$C_{1–5}$	$C_{6–10}$	$C_{11–19}$	$C_{20–40}$	C_{41+}
	Oil-1	Oil-2	Oil-3	Oil-4	Oil-5	Oil-1	Oil-2	Oil-3	Oil-4	Oil-5
	mg HC/g rock					mg HC/g rock				
Sample 1	2.53	6.22	10.58	10.61	17.81	0.03	0.44	4.53	10.61	17.81
Sample 2	1.51	3.71	6.31	6.33	5.48	0.19	1.04	4.43	6.33	5.48
	wt. % (For GW 23 $м^3/м^3$)					wt. %				
Sample 1	5.29	13.03	22.16	22.22	37.29	0	0	6.12	31.1	62.78
Sample 2	6.46	15.90	27.05	27.11	23.47	0	0	17.02	51.92	31.06
Reservoir oil						Reservoir system including bitumen of sample 1				
GW	wt. %					wt. %				
23 m^3/m^3	6.02	14.82	25.20	25.26	28.69	5.29	13.03	22.16	22.22	37.29
53 m^3/m^3	9.58	14.39	24.21	24.26	27.56	8.47	12.72	21.39	21.44	35.99
125 m^3/m^3	17.02	13.51	22.12	22.17	25.18	15.19	12.06	19.74	19.79	33.22

Table 7. Composition of the original reservoir system and the proportion of moving and stationary parts of the original reservoir system

value measured during pyrolysis, which is interpreted as the absence of bitumen in the composition of the original reservoir system. Then we recalculated the dimensional values (mg HC/g rock) into percentages of mobile and immobile HC (bitumen) in the C_{41+} part for two samples (Table 8).

Thus, for sample No. 1, the share of mobile reservoir oil is 87.9%, and bitumen – 12.1%, and for sample No. 2, the share of mobile reservoir oil is 100%, which indicates the absence of heavy bitumen in this interval. This difference in the ratio seems acceptable, since in sample No. 1 the proportion of C_{81+} components is 50.35%, and in sample No. 2 only 21.75%. In the first sample, C_{org} is about 13%, and in the second it is only 2.6%, the OSI parameter (Oil Saturation Index, mg HC/g TOC) is 126 and 293, respectively, which also indicates that the hydrocarbons of sample No. 2 are more mobile. The absence of bitumen in the composition of the initial reservoir system in sample No. 2 is explained by the fact that the bitumoid on which the studies were carried out is parautochthonous, i.e. transported within the oil source strata and not directly related to the place of formation ($\beta_{pyr} = 42.8$). Bitumoid of sample No. 1 contains bitumen of early generation as part of the original reservoir system, since it is syngenetic (autochthonous, β_{pyr} = 26.8).

Knowing the proportions of Oil-1 (C_1–C_5), Oil-2 (C_6–C_{10}) and Oil-3 (C_{11}–C_{19}) in the composition of the original reservoir system, the component composition was calculated using the composition of reservoir mobile oil based on the results of studying recombined samples. The composition for Oil-4 (C_{20}–C_{40}) was determined based on averaging the component compositions of bitumoid No. 1 and reservoir mobile oil for each fraction, the component composition for Oil-5 (C_{41}–C_{81+}) was determined based on the component composition of bitumoid No. 1. Shares Oil-1–Oil-5 in the composition of the initial reservoir hydrocarbon system are given in Table 7.

It is worth noting that this approach makes the assumption that the composition of formation bitumen will not contain components lighter than C_{41+}, although according to the calculation of the adapted PVT model, the composition of formation bitumen (under initial reservoir conditions), which is in thermodynamic equilibrium with formation mobile oil, the proportion of components lighter than C_{40} will be about 14–15 wt. %. To assess the component composition of the initial reservoir system, taking into account the presence of light components and fractions in the bitumen, an adapted PVT model of reservoir oil was used. In the PVT model, the component composition of the initial reservoir system was specified, calculated using the method described above, then the vapor-liquid equilibrium was simulated at the initial reservoir conditions and the compositions of the bitumen and liquid phase were calculated. Further, according to the data on the calculated equilibrium constants between reservoir oil and bitumen, mole fractions of bitumen and oil phases, as well as the composition of reservoir oil based on the results of studying recombined samples, the component composition of the original reservoir system was calculated using formula (11), which is written for the initial reservoir conditions, in this case, the PVT model is adapted to the mass fraction of bitumen in the composition of reservoir oil according to the above analysis:

$$F_b b_i + F_o x_i = z_i,\ b_i = K_i x_i, \tag{11}$$

where F_b is the fraction of the bitumen phase according to the calculation results of the PVT model, mol. %; F_o – fraction of the mobile liquid (oil) phase according to the results of the PVT model calculation, mol. %; b_i – component composition of the bitumen phase, mol. %; x_i – component composition of reservoir oil according to the results of laboratory studies, K_i – equilibrium constants calculated using the PVT model; z_i – component composition of the original reservoir system.

Component compositions determined using the PVT model according to formula (11), as well as by analyzing the data in Table. 7–8 are presented in Appendix A and Fig. 10.

To obtain the exact composition of the initial reservoir system, taking into account bitumen, it is necessary to take a core in a well under pressure with blocking of the reservoir fluid in the core as it rises.

Assessment of the influence of the presence of bitumen on the PVT properties of reservoir mobile oil during reservoir development

Based on the identified component compositions of the initial reservoir hydrocarbon system of the Bazhenov formation, taking into account the bitumen of sample No. 1 and recombined reservoir oil with different gas content,

	Oil-1	Oil-2	Oil-3	Oil-4	Oil-5	Mass fraction %	Molecular Mass. units	ρ (at 20 °C). g/cm^3	β	OSI
	wt. %									
Sample 1 oil	5.29	13.03	22.16	22.22	25.23	87.9				
Sample 1 bitumen	0	0	0	0	12.06	12.1	540.94	1.031	14.27	109
Sample 2 oil	6.47	15.9	27.04	27.12	23.47	**100.0**				
Sample 2 bitumen	0.0	0.0	0.0	0.0	0.0	**0.0**	388.96	0.932	33.25	293

Table 8. Percentages of bitumen in the composition of the initial reservoir system with a gas content of mobile oil of 23 m^3/m^3 and properties of bitumoid

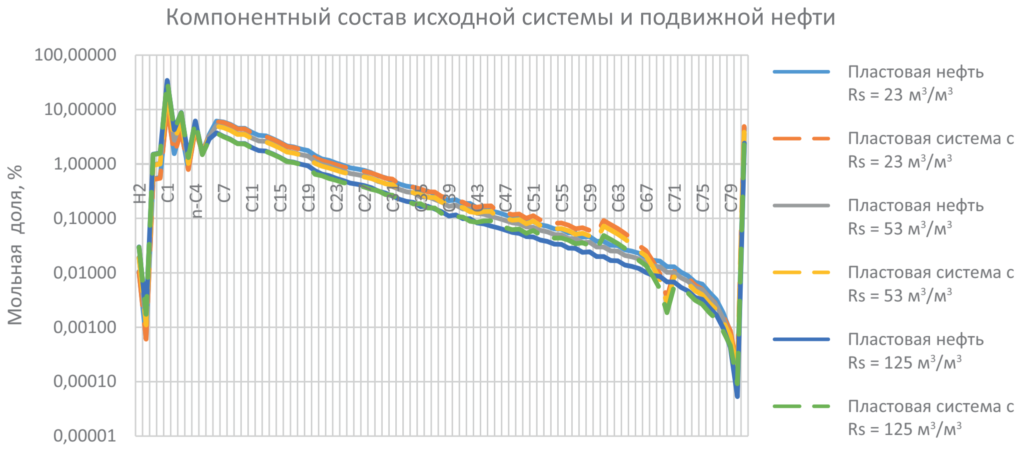

Fig. 10. Component composition of reservoir oil and the initial reservoir hydrocarbon system

their PVT models were created. All parameters of PVT models are similar to PVT models of reservoir oils with different gas content; accordingly, only the component composition has changed.

Next, in the PVT models, the proportion of the solid phase was adapted at the initial reservoir conditions. According to the analysis, the proportion of bitumen for sample No. 1 and reservoir mobile oil is 12.1 wt. %. Modeling of phase equilibrium taking into account the presence of the solid phase was carried out using the cubic three-parameter Peng–Robinson equation of state according to the methods described in (Rydahl et al., 1997; Pedersen, Christensen, 2006). In this case, multiphase equilibrium was calculated according to the algorithms proposed in (Michelsen, Mollerup, 2007, Yushchenko, Brusilovsky, 2016). For PVT models of reservoir oil and PVT models of the original reservoir hydrocarbon system (with the composition presented in Tables 7–8), a phase diagram of vapor-liquid equilibrium was constructed (Fig. 11) and the change in saturation pressure of the liquid phase with gas was estimated. As can be seen from Fig. 11, when taking into account the presence of bitumen in the formation, the saturation pressure of the reservoir oil increases. With increasing gas content, the saturation pressure increases from 1 to 20 bar.

We consider this estimate of the change in saturation pressure to be the maximum possible, since the presence of fractions lighter than C_{40} in bitumen was not taken into account when identifying the component composition of the initial reservoir system. When calculating the composition of the initial reservoir system using formula (11), the phase diagrams do not change significantly.

In the presence of bitumen in the formation, the reservoir mobile oil is extremely saturated with asphaltenes. As the pressure decreases, part of the heavy fractions will move from the liquid phase (reservoir mobile oil) to the solid phase (bitumen), while part of the light fractions will move from the solid phase to mobile oil. In the PVT simulator, the change in the volume fraction of asphaltenes (solid phase) in the reservoir was assessed with a decrease in reservoir pressure, i.e. the process of depletion development of a deposit was simulated. The calculation results are presented in Fig. 12.

According to calculations, the volume of the asphaltene phase increases faster with decreasing pressure for systems with higher gas content. In this case, the solid phase becomes heavier (with a higher content of C_{81+}), and the number of light fractions in it decreases. The saturation pressure of oil with gas in the process of pressure reduction changes insignificantly (less than 1% for all three systems with different gas content). A decrease in pressure leads to a decrease in the volume of the mobile phase and pore volume due to phase transformations and, thus, negatively affects the accumulated hydrocarbon production in the process of depletion development of the reservoir.

In addition to assessing changes in the PVT properties of the liquid hydrocarbon phase in the formation in systems with and without bitumen, PVT modeling of the effect of the presence of bitumen on the intensification of production using EOR was also carried out.

In the first case, a comparison was made of APG injection for PVT models of reservoir oil with and without taking into account bitumen. Using PVT modeling, swelling and slim tube experiments were carried out for reservoir oil and the original reservoir system, taking into account bitumen. The simulation results are shown in Fig. 13.

Based on the results of the simulation of the swelling experiment, it can be concluded that taking into account the presence of bitumen will affect the change in the volume of the liquid phase when the injected gas is dissolved in it (for oil without taking into account bitumen, the volume expansion is faster), but at the same time the saturation pressure of the liquid phase in the presence of bitumen higher. Accordingly, the amount of dissolved gas with and without bitumen in the limiting case will be almost the same. The minimum miscibility

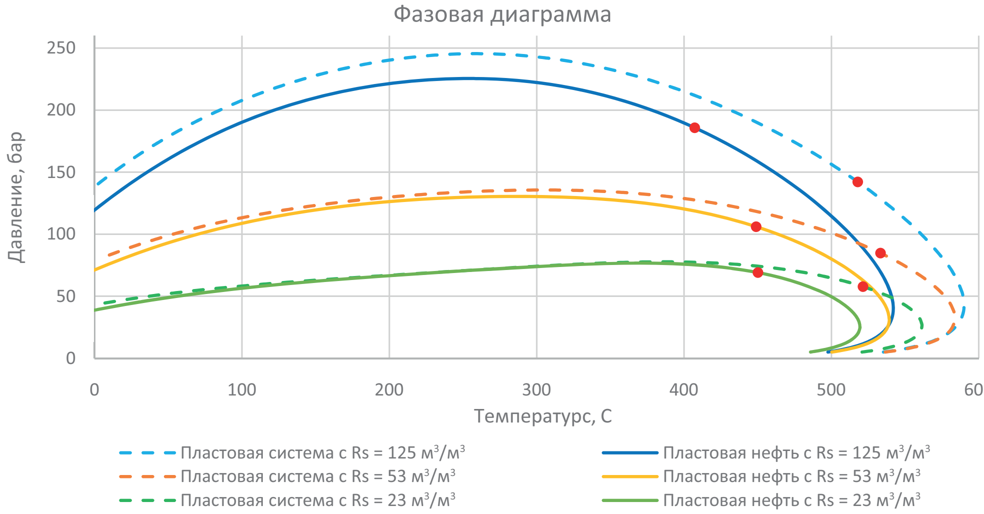

Fig. 11 Vapor-liquid phase diagram of reservoir oil and the original reservoir system, constructed using PVT model

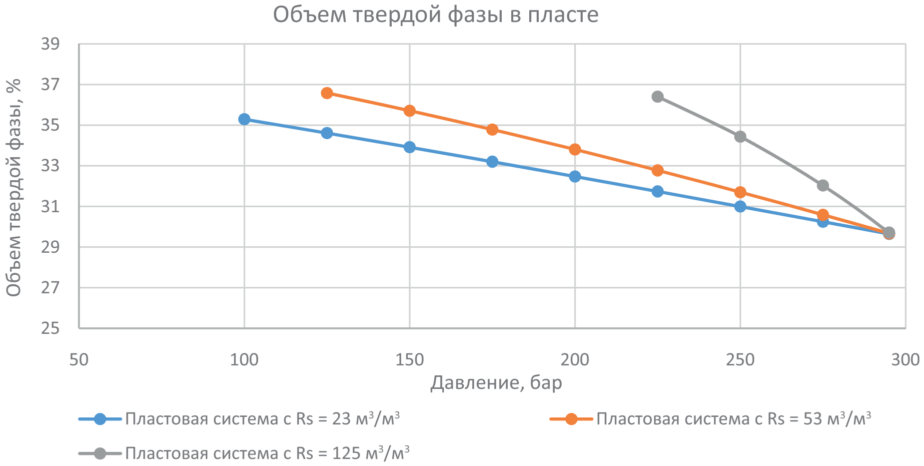

Fig. 12. Change in the proportion of asphaltenes (a separate solid phase) in the PVT model with a decrease in reservoir pressure

pressure for reservoir oil during APG injection is not achieved at pressures not exceeding reservoir pressure for both reservoir oil and the reservoir system taking into account bitumen.

In the second case, calculations were carried out of the influence of thermal EOR on the behavior of the formation fluid both in the presence of bitumen and without it in the formation. An assessment was made of changes in the composition and properties of the liquid phase (reservoir oil) when heating a reservoir system with bitumen using PVT modeling. It should be noted that the processes of oxidation and sorption were not taken into account in the calculations; only the phase behavior and changes in the thermodynamic properties of fluids were taken into account. The simulation results are presented in Fig. 14.

When the reservoir hydrocarbon system is heated, the proportion of asphaltenes (solid phase) decreases significantly, because some of the heavy components pass into the liquid phase. Note that the behavior of a reservoir system with a gas content of 23 m^3/m^3 differs from reservoir systems with a higher gas content: the viscosity of the reservoir oil phase when heated from 100 °C to 150 °C increases slightly, and then only begins to decrease. For reservoir systems with higher gas content, the viscosity of the reservoir oil phase decreases as it heats up, while the volume of the bitumen phase does not decrease so significantly.

Based on the results of calculations for heating reservoir systems taking into account bitumen, it can be assumed based on PVT modeling that thermal EOR is most effective for systems with low gas content. At the same time, the significant positive effect of EOR on oil production is noticeable for all reservoir systems under consideration. To confirm this effect, hydrodynamic studies are required.

We note the lack of tuning of the PVT model to the properties of bitumen at initial reservoir conditions. For a more correct calculation, laboratory studies are required to obtain experimental data on the phase equilibria of bitumen and mobile oil.

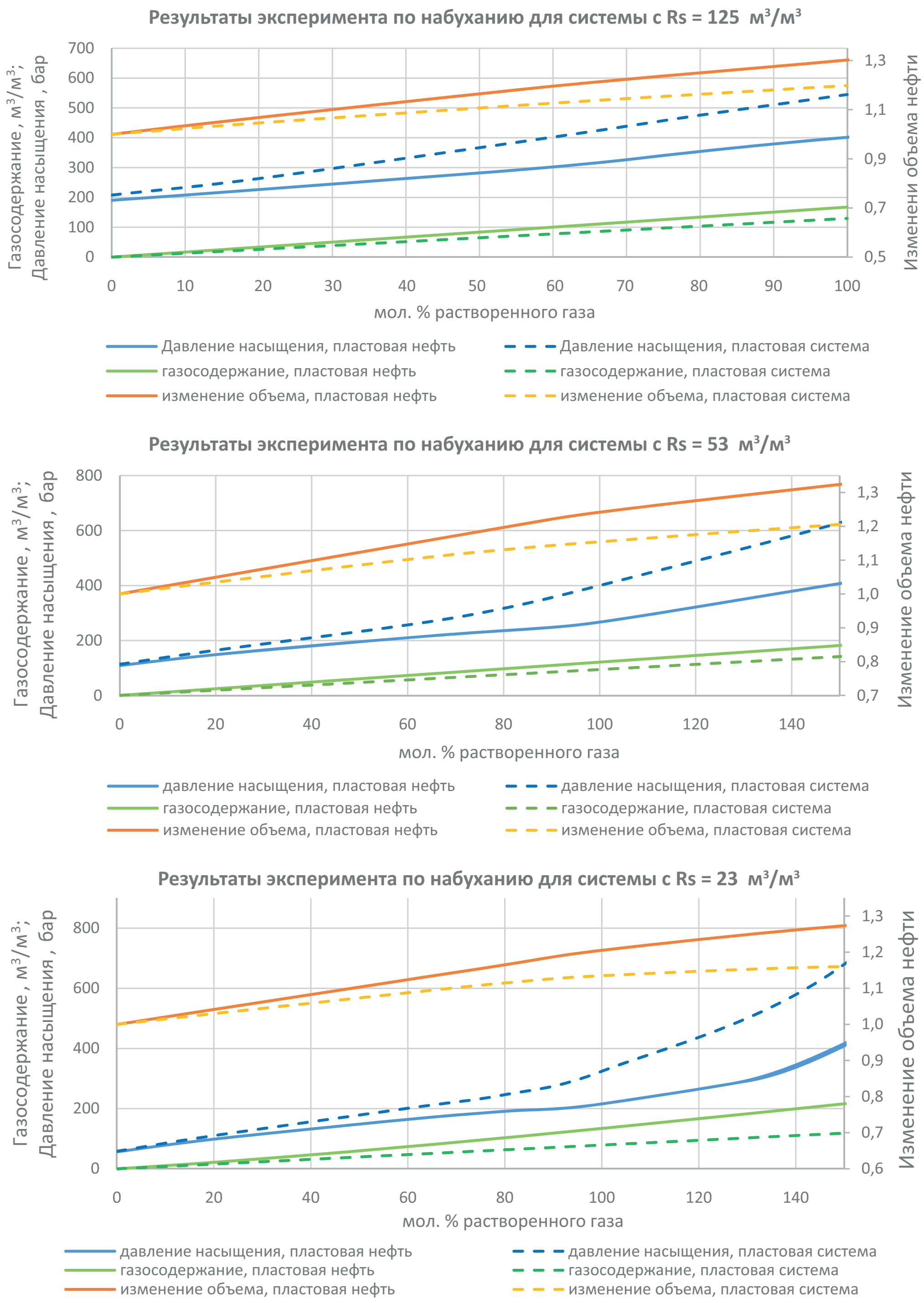

Fig. 13. Simulation in the PVT model of a swelling test for reservoir oil with and without taking into account bitumen

Conclusion

The work describes in detail the method for identifying the component composition of the reservoir hydrocarbon system of the Bazhenov formation, taking into account the presence of heavy immobile hydrocarbons (bitumen) in the reservoir. Based on laboratory studies, analysis of their results and PVT modeling, a new approach has been developed to assess changes in the component composition and PVT properties of the formation moving fluid in the presence of bitumen in the formation during the development of the deposit. The proposed approach was tested using the example of a reservoir system of one of the wells of the Bazhenov formation. This approach is a combination of geochemical research methods and PVT modeling, which allows a more comprehensive approach to solving the problem of identifying high-molecular hydrocarbon compounds in shale deposits and assessing their impact on development.

As a result of the PVT modeling, it was shown that the presence of bitumen in the formation has virtually no effect on the PVT properties of the mobile phase.

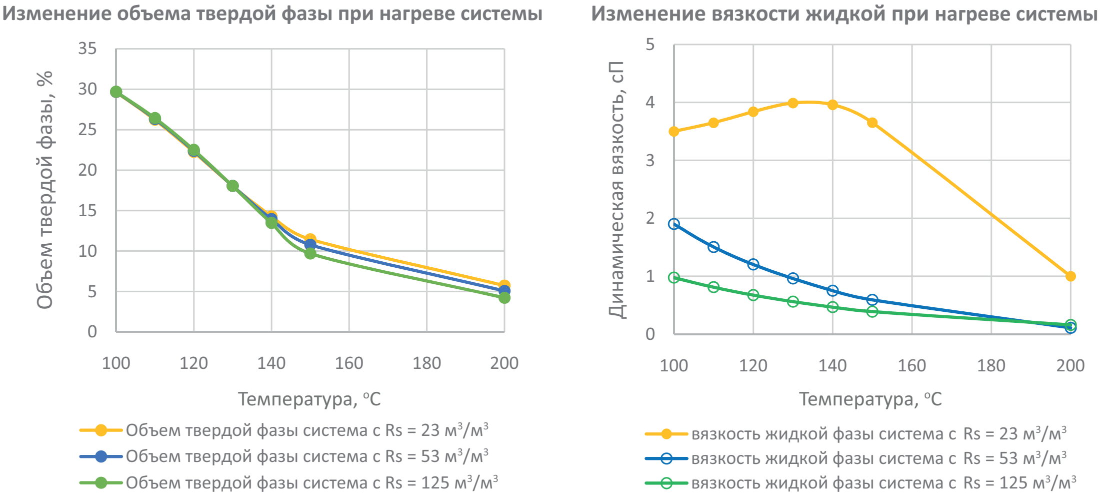

Fig. 14. Change in the volume of the solid phase and viscosity of the mobile phase when the system is heated

A decrease in pressure leads to an increase in the volume of bitumen in the formation, and an increase in temperature, on the contrary, leads to a significant decrease in its volume.

To more accurately determine the effect of bitumen on the behavior of reservoir oil, laboratory studies in the PVT cell of the original reservoir hydrocarbon system are required.

Assumptions

In this study, the processes of desorption in the formation during pressure reduction were not taken into account. This effect is planned to be taken into account in future work. When assessing the influence of bitumen on the PVT properties of the reservoir system, the proportion and properties of the asphaltene (solid phase) were calculated based on the Peng–Robinson equation of state using solid phase modeling methods. Laboratory PVT studies of the properties of the reservoir system were also not carried out, assuming the presence of bitumen in the PVT cell.

References

Abrams M.A., Gong C., Garnier C., Sephton M.A. (2017). A new thermal extraction protocol to evaluate liquid rich unconventional oil in place and in-situ fluid chemistry. *Marine and Petroleum Geology*, 88, pp. 659–675. https://doi.org/10.1016/j.marpetgeo.2017.09.014

Al Solial A.J., Shaikh A., Idrees A.K. (2023). Identification and Mapping of Gas Reservoir Bitumen. *Middle East Oil, Gas and Geosciences Show*, SPE-213390-MS. https://doi.org/10.2118/213390-MS

Beti D.R., Ring T.A. (2019). Programmed temperature pyrolysis: Alterations to the standard method. *Sorkhabi R. (ed.) Encyclopedia of Petroleum Geoscience. Encyclopedia of Earth Sciences Series*. Springer, Cham., pp. 1–12. https://doi.org/10.1007/978-3-319-02330-4_302-1

Brusilovsky A.I. (2002). Phase transformations during the development of oil and gas fields. Moscow: Grail, 575 p. (In Russ.)

Chen S., Fan X., Lu J., Wang X., Fei A. (2010). Impact of bitumen on reservoir properties and hydrocarbon accumulation. *Petroleum Exploration and Development*, 37(1), 1793-0, pp. 70–76.

Cheremisin A.N., Mukhina E.D., Ushakova A.S., Prochukhan K.Yu., Kasyanenko A.A. (2022). Chemical, gas and thermal EOR for the Bazhenov formation. *Neftegaz.ru*, 5–6, pp. 58-64. (In Russ.)

Gomaa S., El-Hosboudy A.N. (2018). New Correlation Predicting Molecular Weight of Petroleum Fractions. *Petroleum & Petrochemical Engineering Journal*, 2(1), pp. 1–5. https://doi.org/10.23880/PPEJ-16000139

Gutman I.S., Potemkin G.N., Baturin A.Yu., Maslyanko M.Yu., Kozlova E.V., Spasennykh M.Yu., Bulatov T.D. (2019). Study of the West Siberian Bazhenov Formation at multiple levels according to pyrolysis data as the basis for the unbiased assessment of petroleum potential. *Nedropolzovanie XXI vek*, 79(3), pp. 102–115. (In Russ.)

Handbook of Oil and Gas Geology (1984). Ed. N.A. Eremenko. Moscow: Nedra, 480 p. (In Russ.)

Kalmykov G.A. (2016). The structure of the Bazhenov oil and gas complex as the basis for forecasting differentiated oil productivity. Dr. Geol. and Mineral. Sci. Diss. Moscow: MSU. (In Russ.)

Katz D.L., Firoozabadi A. (1978). Predicting Phase Behavior of Condensate/Crude-Oil Systems Using Methane Interaction Coefficients. *Journal of Petroleum Technology*, 30(11), SPE-6721-PA, pp. 1649–1655. https://doi.org/10.2118/6721-PA

Kontorovich A.E., Kostyreva E.A., Rodyakin S.V., Sotnich I.S. and others (2018). Geochemistry of bitumens of the Bazhenov formation. *Geologiya nefti i gaza = Russian Oil and Gas Geology*, 2, pp. 79–88. (In Russ.)

Kontorovich A.E., Melenevsky V.N., Zanin Yu.N., Zamirailova A.G., Kazanenkov V.A., Kazarbin V.V., Makhneva E.N., Yamkovaya L.S. (1998). Lithology, organic geochemistry and conditions for the formation of the main types of rocks of the Bazhenov Formation. *Geologiya i Geofizika,* 39 (11), pp. 1477–1491. (In Russ.)

Kozlova E.V., Fadeeva N.P., Kalmykov G.A., Balushkina N.S. and others (2015). Technology for studying the geochemical parameters of organic matter in kerogen-saturated sediments (using the example of the Bazhenov formation, Western Siberia). *Moscow University Bulletin. Series 4. Geology*, 5, pp. 44–53. (In Russ.)

Kulkov M.G., Vtorushina E.A. (2019). Accelerated extraction ASE – as an effective method for extracting bitumen when performing pyrolytic and chromatographic studies of core material. *Ways to realize the oil and gas potential of the Khanty-Mansiysk Autonomous Okrug – Ugra: Proc. Sci and Pract. Conf.* Khanty-Mansiysk: V.I. Shpilman Research and Analytical Centre for the Rational Use of the Subsoil, pp. 79–90. (In Russ.)

Lee B.I., Kesler M.G. (1975). A Generalized Thermodynamic Correlation Based on Three-Parameter Corresponding States. *AIChE Journal*, 21(3), pp. 510–527. https://doi.org/10.1002/aic.690210313

Lopatin N.V., Yemets T.P. (1999). Oil generation properties of the Bazhenov formation on the territory of the Khanty-Mansiysk Autonomous Okrug. *Ways to realize the oil and gas potential of the Khanty-Mansiysk Autonomous Okrug – Ugra: Proc. Sci and Pract. Conf.* Khanty-Mansiysk, pp. 116–123. (In Russ.)

Maende A., Pepper A., Jarvie D.M., Weldon W.D. (2017). Advanced pyrolysis data and interpretation methods to identify unconventional reservoir sweet spots in fluid phase saturation and fluid properties (API gravity) from drill cuttings and cores. *AAPG 2017 Annual Convention & Exhibition, Houston, Texas,* https://www.searchanddiscovery.com/pdfz/documents/2017/80596maende/ndx_maende.pdf.html

Michelsen M.L., Mollerup J. (2007). Thermodynamic Models: Fundamentals and Computational Aspects. Denmark: Tie-Line Publ., 382 p.

Muradov A.V., Dieva N.N., Kravchenko M.N., Perekhozhev F.A. (2018). HSV and THCV in the formations of the Bazhenov formation. *Neftegaz.Ru,* 3, pp. 62–69. (In Russ.)

Naji H.S. (2010). Characterizing Pure and Undefined Petroleum Components. *International Journal of Engineering and Technology IJET-IJENS*, 10(2), pp. 39–68.

Pedersen K.S., Christensen P.L. (2006). Phase Behavior of Petroleum Reservoir Fluids. Boca Raton: CRC Press, 422 p. https://doi.org/10.1201/9781420018257

Péneloux A., Rauzy E., Fréze R. (1982). A consistent volume correction for Redlich–Kwong–Soave volumes. *Fluid Phase Equilibria*, 8(1), pp. 7–23. https://doi.org/10.1016/0378-3812(82)80002-2

Peng D.-Y., Robinson D.B. (1976). A new Two-Constant Equation of state. *Industrial & Engineering Chemistry Fundamentals*, 15(1), pp. 59–64. https://doi.org/10.1021/i160057a011

Peters K.E., Cassa M.R. (1994). Applied source rock geochemistry. *Magoon L.B., Dow W.G. The Petroleum System – From Source to Trap*. AAPG, pp. 93–120. https://doi.org/10.1306/M60585C5

Riazi M.R., Al-Sahhaf T.A. (1996). Physical Properties of Heavy Petroleum Fractions and Crude Oils. *Fluid Phase Equilibria*, 117(1–2), pp. 217–224. https://doi.org/10.1016/0378-3812(95)02956-7

Rydahl A., Pedersen K.S., Hjermstad H.P. (1997). Modelling of Live Oil Asphaltene Precipitation. *AIChE Spring National Meeting*, Houston, TX, USA.

Salakhidinova G.T., Kulkov M.G., Vtorushina E.A. (2022). Increasing the reliability of assessing the degree of catagenesis of organic matter of the Bazhenov Formation by combining pyrolytic and molecular parameters (within the northwestern part of the territory of the Khanty-Mansiysk Autonomous Okrug – Ugra). *Geologiya nefti i gaza = Russian Oil and Gas Geology*, 6, pp. 85–99. (In Russ.)

Samoilenko V.V. (2011). Geochemistry of organic matter of the Bazhenov formation in the southeast of Western Siberia and genetically related fluids. Abstract Cand. Geol. and Mineral. Sci. Diss. Tomsk, 22 p. (In Russ.)

Soboleva E.V. (2017). Formation of the oil composition of the Yu0 Bazhenov formation, Salym oil field. *Georesursy = Georesources*, Special issue, pp. 144–154. (In Russ.) http://doi.org/10.18599/grs.19.15

Spasennykh M., Maglevannaia P., Kozlova E., Bulatov T., Leushina E., Morozov N. (2021). Geochemical Trends Reflecting Hydrocarbon Generation, Migration and Accumulation in Unconventional Reservoirs Based on Pyrolysis Data (on the Example of the Bazhenov Formation). *Geosciences*, 11(8), 307. https://doi.org/10.3390/geosciences11080307

Tikhonova M.S., Ivanova D.A., Kalmykov A.G., Borisov R.S., Kalmykov G.A. (2019). Methods of step extraction of rocks of high-carbon formations for the study of the component distribution of bitumen and variability of their basic geochemical parameters. *Georesursy = Georesources*, 21(2), pp. 172–182. https:// doi.org/10.18599/grs.2019.2.172-182

Ugryumov A., Petrova D., Sannikova I., Kasyanenko A., Khachaturyan M., Kolomytsev A., Yuschenko T., Plotnikov B., Karimov I. (2022). Prospectivity Assessment of Bazhenov Formation Using Cutting-edge Integrated Static Model. *SPE/AAPG/SEG Unconventional Resources Technology Conference*, URTEC-3723536-MS. https://doi.org/10.15530/urtec-2022-3723536

Uspensky V.A., Rodionova K.F., Gorskaya A.I., Shishkova A.P. (1966). Guide to the analysis of bitumen and dispersed organic matter of rocks (for laboratories of geological exploration organizations). Leningrad: Nedra, 316 p. (In Russ.)

Volkov V.A., Oleinik E.V., Oksenoid E.E., Sidorov A.A. (2016). Structure and generation potential of the Bazhenov Formation in the central part of Western Siberia. *Geologiya i mineral’no-syr’evye resursy*, 3(27), pp. 79–98. (In Russ.)

Vtorushina E.A., Bulatov T.D., Kozlova E.V., Kulkov M.G. (2022). Pyrolytic criteria for assessing the degree of thermal maturity of organic matter of the Bazhenov Formation. *Geologiya nefti i gaza = Russian Oil and Gas Geology*, 4, pp. 53–63. (In Russ.)

Whitson C.H., Brulé M.R. (2000). Phase Behavior. SPE, 239 p. https://doi.org/10.2118/9781555630874

Yushchenko T.S., Brusilovsky A.I. (2016). Mathematical modeling of gas-condensate mixture PVT-properties including presence of brine in reservoir. *Fluid Phase Equilibria*, 409, pp. 37–48. https://doi.org/10.1016/j.fluid.2015.09.029

Yushchenko T.S., Brusilovsky A.I. (2022). A step-by-step approach to creating and tuning PVT-models of reservoir hydrocarbon systems based on the state equation. *Georesursy = Georesources,* 24(3), pp. 164–181. (In Russ.) https://doi.org/10.18599/grs.2022.3.14

About the Authors

Taras S. Yushchenko – Cand. Sci. (Physics and Mathematics), Head of PVT and Well Operations, Gazprom Neft

3-5, Litera A, Pochtamtskaya st., St. Petersburg, 190000, Russian Federation

e-mail: Yuschenko.TS@gazprom-neft.ru

Irina A. Sannikova – Cand. Sci. (Geology and Mineralogy), Chief Specialist, Gazprom Neft

3-5, Litera A, Pochtamtskaya st., St. Petersburg, 190000, Russian Federation

e-mail: Sannikova.IA@gazprom-neft.ru

Mikhail G. Kulkov – Head of the Laboratory of Chromatographic Research Methods, V.I. Shpilman Research and Analytical Centre for the Rational Use of the Subsoil

2, Studencheskaya st., Khanty-Mansiysk, 628011, Russian Federation

e-mail: KulkovMG@nacrn.hmao.ru

Alexander I. Brusilovskiy – Dr. Sci. (Technical Sciences), Professor, Leading Expert, Gazprom Neft

3-5, Litera A, Pochtamtskaya st., St. Petersburg, 190000, Russian Federation

e-mail: Brusilovskiy.AI@gazprom-neft.ru

Gulmira T. Salakhidinova – Cand. Sci. (Geology and Mineralogy), Senior Researcher at the Laboratory of Chromatographic Research Methods, V.I. Shpilman Research and Analytical Centre for the Rational Use of the Subsoil

2, Studencheskaya st., Khanty-Mansiysk, 628011, Russian Federation

e-mail: SalakhidinovaGT@nacrn.hmao.ru

Azim Enverovich Aliev – Engineer of the lLaboratory of Chromatographic Research Methods, V.I. Shpilman Research and Analytical Centre for the Rational Use of the Subsoil

2, Studencheskaya st., Khanty-Mansiysk, 628011, Russian Federation

e-mail: AlievAE@nacrn.hmao.ru

Aleksandr E. Gavrilov – Head of the Department, Gazprom Neft

3-5, Litera A, Pochtamtskaya st., St. Petersburg, 190000, Russian Federation

e-mail: Gavrilov.AE@gazprom-neft.ru

Manuscript received 27 April 2023;
Accepted 31 January 2024; Published 30 March 2024

Appendix A. Component composition of separated oil, bitumoids, recombined samples of reservoir oil and original reservoir systems of the Bazhenov formation (mol %). Designation: GOR – gas oil ratio.

Компонент/ фракция	Молярная масса, г/моль	Битумоид № 1	Битумоид № 2	Сепарированная нефть	Устьевой газ	Рекомбинированная нефть с ГС 23 м^3/м^3	Рекомбинированная нефть с ГС 53 м^3/м^3	Рекомбинированная нефть с ГС 125 м^3/м^3	Расчет по данным табл. 7 и 8			Согласно PVT-модель (11)		
									Исходная пластовая система с ГС 23 м^3/м^3	Исходная пластовая система с ГС 53 м^3/м^3	Исходная пластовая система с ГС 125 м^3/м^3	Исходная пластовая система с ГС 23 м^3/м^3	Исходная пластовая система с ГС 53 м^3/м^3	Исходная пластовая система с ГС 125 м^3/м^3
H_2	2	0	0	0	0,051	0,011	0,019	0,030	0,010	0,019	0,029	0,010	0,018	0,028
He	4	0	0	0	0,003	0,001	0,001	0,002	0,001	0,001	0,002	0,001	0,001	0,002
N_2	28	0	0	0	2,577	0,534	0,967	1,507	0,519	0,945	1,487	0,503	0,916	1,442
CO_2	44	0	0	0	2,715	0,563	1,019	1,587	0,547	0,996	1,566	0,545	0,988	1,555
C_1	16,04	0,000	0,000	0	58,69	12,16	22,02	34,31	11,814	21,524	33,860	11,793	21,368	33,635
C_2	30,07	0,000	0,000	0,071	7,230	1,554	2,757	4,256	1,510	2,695	4,200	1,497	2,659	4,146
C_3	44,1	0,000	0,000	1,537	13,95	4,109	6,194	8,792	3,991	6,054	8,676	3,984	6,010	8,621
i-C_4	58,12	0,000	0,000	0,527	1,905	0,813	1,044	1,333	0,789	1,020	1,315	0,790	1,017	1,311
nC_4	58,12	0,000	0,000	3,571	7,989	4,487	5,229	6,154	4,358	5,110	6,073	4,363	5,091	6,054
i-C_5	72,15	0,000	0,000	1,737	1,349	1,656	1,591	1,510	1,609	1,555	1,490	1,598	1,541	1,477
nC_5	72,15	0,000	0,000	3,863	2,182	3,515	3,232	2,880	3,414	3,159	2,842	3,391	3,130	2,818
C_6	84	0,000	0,000	7,486	1,068	6,156	5,078	3,734	5,980	4,963	3,685	5,917	4,916	3,653
C_7	96	0,000	0,000	7,429	0,211	5,933	4,720	3,209	5,763	4,614	3,167	5,703	4,571	3,139
C_8	107	0,000	0,000	6,720	0,080	5,344	4,228	2,838	5,191	4,133	2,801	5,088	4,066	2,758
C_9	121	0,000	0,000	5,720	0,008	4,537	3,577	2,381	4,407	3,496	2,350	4,319	3,440	2,313
C_{10}	134	0,000	0,000	5,725	0,000	4,539	3,577	2,378	4,409	3,496	2,347	4,282	3,418	2,296
C_{11}	154,21	0,000	0,013	4,840	0,000	3,837	3,024	2,010	3,727	2,954	1,984	3,620	2,889	1,941
C_{12}	168,2	0,000	0,003	4,244	0,000	3,364	2,651	1,763	3,268	2,590	1,740	3,142	2,516	1,690
C_{13}	182,31	0,000	0,000	4,165	0,000	3,302	2,602	1,730	3,207	2,542	1,708	3,085	2,469	1,658
C_{14}	197,23	0,000	0,117	3,678	0,000	2,916	2,298	1,528	2,832	2,245	1,508	2,724	2,180	1,465
C_{15}	211,28	0,432	1,422	3,198	0,000	2,535	1,998	1,328	2,463	1,952	1,311	2,344	1,882	1,263
C_{16}	225,11	1,462	3,892	2,713	0,000	2,151	1,695	1,127	2,089	1,656	1,112	1,989	1,596	1,072
C_{17}	238,61	2,891	6,251	2,590	0,000	2,053	1,618	1,076	1,995	1,581	1,062	1,898	1,524	1,023
C_{18}	251,68	4,093	7,529	2,380	0,000	1,887	1,487	0,989	1,833	1,453	0,976	1,727	1,390	0,934
C_{19}	265,21	4,421	7,656	2,232	0,000	1,770	1,395	0,927	1,719	1,363	0,915	1,620	1,304	0,876
C_{20}	279,18	4,262	6,590	1,815	0,000	1,439	1,134	0,754	1,290	1,022	0,649	1,317	1,060	0,712
C_{21}	291,52	3,944	6,012	1,563	0,000	1,239	0,977	0,649	1,149	0,911	0,606	1,134	0,913	0,613
C_{22}	305,26	3,574	5,316	1,469	0,000	1,165	0,918	0,610	1,061	0,841	0,542	1,057	0,853	0,573
C_{23}	317,19	3,335	4,762	1,308	0,000	1,037	0,817	0,543	0,966	0,766	0,500	0,940	0,759	0,510
C_{24}	329,39	3,045	4,367	1,193	0,000	0,946	0,745	0,496	0,881	0,699	0,453	0,858	0,692	0,465
C_{25}	341,85	2,971	3,849	1,072	0,000	0,850	0,670	0,445	0,825	0,654	0,435	0,771	0,622	0,418
C_{26}	353,41	2,757	3,655	1,020	0,000	0,808	0,637	0,424	0,775	0,614	0,407	0,728	0,589	0,396
C_{27}	365,2	2,594	3,474	0,961	0,000	0,762	0,600	0,399	0,729	0,578	0,376	0,686	0,555	0,372
C_{28}	374,77	2,452	2,919	0,880	0,000	0,698	0,550	0,366	0,679	0,538	0,342	0,628	0,508	0,341
C_{29}	386,94	2,320	2,623	0,763	0,000	0,605	0,477	0,317	0,615	0,488	0,320	0,544	0,441	0,296
C_{30}	398,06	1,980	2,218	0,706	0,000	0,560	0,441	0,293	0,546	0,433	0,276	0,501	0,406	0,273
C_{31}	409,35	2,077	1,957	0,618	0,000	0,490	0,386	0,257	0,526	0,417	0,267	0,438	0,355	0,239
C_{32}	419,53	1,522	1,632	0,543	0,000	0,431	0,339	0,226	0,420	0,333	0,216	0,385	0,312	0,210
C_{33}	429,83	1,567	1,498	0,494	0,000	0,392	0,309	0,205	0,407	0,323	0,215	0,350	0,284	0,190
C_{34}	438,95	1,378	1,251	0,474	0,000	0,376	0,296	0,197	0,373	0,296	0,185	0,335	0,272	0,183
C_{35}	449,48	1,398	1,162	0,396	0,000	0,314	0,248	0,165	0,346	0,275	0,187	0,281	0,228	0,153
C_{36}	458,8	1,103	1,063	0,401	0,000	0,318	0,251	0,167	0,307	0,244	0,156	0,283	0,230	0,155

Компонент/ фракция	Молярная масса, г/моль	Битумоид № 1	Битумоид № 2	Сепарированная нефть	Устьевой газ	Рекомбинированная нефть с ГС 23 м^3/м^3	Рекомбинированная нефть с ГС 53 м^3/м^3	Рекомбинированная нефть с ГС 125 м^3/м^3	Расчет по данным табл. 7 и 8			Согласно PVT-модель (11)		
									Исходная пластовая система с ГС 23 м^3/м^3	Исходная пластовая система с ГС 53 м^3/м^3	Исходная пластовая система с ГС 125 м^3/м^3	Исходная пластовая система с ГС 23 м^3/м^3	Исходная пластовая система с ГС 53 м^3/м^3	Исходная пластовая система с ГС 125 м^3/м^3
C$_{37}$	468,2	1,201	0,938	0,359	0,000	0,284	0,224	0,149	0,305	0,241	0,155	0,253	0,205	0,138
C$_{38}$	476,34	0,922	0,778	0,319	0,000	0,253	0,199	0,133	0,251	0,199	0,124	0,225	0,182	0,123
C$_{39}$	485,91	1,011	0,709	0,267	0,000	0,212	0,167	0,111	0,243	0,193	0,133	0,188	0,153	0,103
C$_{40}$	494,18	0,800	0,648	0,279	0,000	0,221	0,174	0,116	0,214	0,173	0,109	0,197	0,160	0,107
C$_{41}$	502,51	0,860	0,573	0,238	0,000	0,189	0,149	0,099	0,198	0,157	0,106	0,169	0,137	0,093
C$_{42}$	510,91	0,724	0,524	0,238	0,000	0,188	0,148	0,099	0,167	0,132	0,089	0,169	0,137	0,092
C$_{43}$	519,36	0,694	0,489	0,199	0,000	0,158	0,124	0,083	0,160	0,127	0,085	0,141	0,115	0,077
C$_{44}$	526,45	0,731	0,445	0,190	0,000	0,151	0,119	0,079	0,168	0,133	0,090	0,135	0,110	0,073
C$_{45}$	533,58	0,737	0,401	0,173	0,000	0,137	0,108	0,072	0,170	0,135	0,090	0,123	0,100	0,067
C$_{46}$	542,19	0,552	0,335	0,161	0,000	0,128	0,100	0,067	0,127	0,101	0,068	0,114	0,093	0,062
C$_{47}$	549,41	0,555	0,317	0,147	0,000	0,116	0,092	0,061	0,128	0,101	0,068	0,104	0,085	0,057
C$_{48}$	556,66	0,507	0,290	0,133	0,000	0,105	0,083	0,055	0,117	0,093	0,062	0,096	0,078	0,052
C$_{49}$	562,49	0,522	0,285	0,127	0,000	0,101	0,080	0,053	0,120	0,095	0,064	0,092	0,075	0,050
C$_{50}$	569,81	0,435	0,242	0,111	0,000	0,088	0,070	0,046	0,100	0,079	0,053	0,081	0,065	0,044
C$_{51}$	575,69	0,487	0,214	0,110	0,000	0,087	0,069	0,046	0,112	0,089	0,060	0,080	0,064	0,043
C$_{52}$	583,07	0,406	0,228	0,096	0,000	0,076	0,060	0,040	0,093	0,074	0,050	0,070	0,056	0,038
C$_{53}$	589	0,431	0,211	0,091	0,000	0,072	0,057	0,038	0,099	0,079	0,053	0,066	0,053	0,036
C$_{54}$	594,96	0,354	0,166	0,081	0,000	0,064	0,051	0,034	0,082	0,065	0,044	0,059	0,047	0,032
C$_{55}$	600,93	0,357	0,176	0,080	0,000	0,063	0,050	0,033	0,082	0,065	0,044	0,059	0,047	0,032
C$_{56}$	606,92	0,325	0,156	0,068	0,000	0,054	0,043	0,028	0,075	0,059	0,040	0,051	0,040	0,027
C$_{57}$	612,94	0,280	0,135	0,068	0,000	0,054	0,042	0,028	0,064	0,051	0,034	0,049	0,040	0,026
C$_{58}$	618,97	0,292	0,163	0,057	0,000	0,045	0,036	0,024	0,067	0,053	0,036	0,042	0,033	0,022
C$_{59}$	625,02	0,260	0,130	0,058	0,000	0,046	0,036	0,024	0,060	0,047	0,032	0,042	0,034	0,023
C$_{60}$	629,58	0,219	0,109	0,048	0,000	0,038	0,030	0,020	0,051	0,040	0,027	0,035	0,028	0,019
C$_{61}$	635,66	0,395	0,101	0,048	0,000	0,038	0,030	0,020	0,091	0,072	0,049	0,035	0,028	0,019
C$_{62}$	640,24	0,333	0,094	0,040	0,000	0,032	0,025	0,017	0,077	0,061	0,041	0,029	0,024	0,016
C$_{63}$	644,83	0,281	0,082	0,040	0,000	0,032	0,025	0,017	0,065	0,051	0,034	0,030	0,024	0,016
C$_{64}$	650,96	0,229	0,073	0,034	0,000	0,027	0,021	0,014	0,053	0,042	0,028	0,025	0,020	0,013
C$_{65}$	655,57	0,181	0,069	0,031	0,000	0,025	0,020	0,013	0,042	0,033	0,022	0,023	0,019	0,013
C$_{66}$	660,19	0,138	0,058	0,029	0,000	0,023	0,018	0,012	0,032	0,025	0,017	0,022	0,017	0,011
C$_{67}$	664,82	0,112	0,055	0,025	0,000	0,019	0,015	0,010	0,026	0,020	0,014	0,018	0,015	0,010
C$_{68}$	669,45	0,070	0,050	0,021	0,000	0,017	0,013	0,009	0,016	0,013	0,009	0,016	0,013	0,009
C$_{69}$	674,1	0,041	0,042	0,021	0,000	0,016	0,013	0,009	0,009	0,007	0,005	0,015	0,012	0,008
C$_{70}$	678,76	0,015	0,037	0,016	0,000	0,013	0,010	0,007	0,003	0,003	0,002	0,012	0,010	0,007
C$_{71}$	683,42	0,046	0,033	0,016	0,000	0,013	0,010	0,007	0,011	0,008	0,006	0,013	0,010	0,007
C$_{72}$	688,09	0,038	0,027	0,013	0,000	0,010	0,008	0,005	0,009	0,007	0,005	0,010	0,008	0,005
C$_{73}$	691,21	0,035	0,025	0,011	0,000	0,009	0,007	0,005	0,008	0,006	0,004	0,009	0,007	0,005
C$_{74}$	695,9	0,026	0,019	0,009	0,000	0,007	0,005	0,004	0,006	0,005	0,003	0,007	0,005	0,004
C$_{75}$	700,59	0,022	0,016	0,008	0,000	0,006	0,005	0,003	0,005	0,004	0,003	0,006	0,005	0,003
C$_{76}$	705,3	0,016	0,011	0,006	0,000	0,004	0,003	0,002	0,004	0,003	0,002	0,004	0,004	0,002
C$_{77}$	710,01	0,011	0,008	0,004	0,000	0,003	0,003	0,002	0,003	0,002	0,001	0,003	0,003	0,002
C$_{78}$	714,72	0,007	0,005	0,002	0,000	0,002	0,001	0,001	0,002	0,001	0,001	0,002	0,001	0,001
C$_{79}$	719,45	0,004	0,003	0,001	0,000	0,001	0,001	0,000	0,001	0,001	0,000	0,001	0,001	0,000
C$_{80}$	722,6	0,001	0,001	0,000	0,000	0,000	0,000	0,000	0,000	0,000	0,000	0,001	0,000	0,000
C$_{81+}$	904	28,760	9,300	5,819	0,000	4,613	3,635	2,417	6,944	5,505	3,697	9,891	7,656	5,143

*Appendix B. Katz-Firoozabadi table, expanded to the C_{80} fraction. *At a pressure of 0.101325 MPa.*

Номер фракции	Температура кипения*, °C	Относительная плотность	Молекулярная масса	Коэффициент Ватсона	Методика (Ющенко, Брусиловский, 2022)		
	Среднее значение				Критическая температура, °C	Критическое давление, бар	Ацентрический фактор
6	63,9	0,698	85,2	12,27	249,38	32,77	0,267
7	91,9	0,726	98,8	11,96	278,64	30,35	0,317
8	116,7	0,745	112,2	11,86	305,24	28,26	0,364
9	142,2	0,759	126,5	11,82	330,44	26,27	0,413
10	174,0	0,786	133,4	11,82	348,53	26,37	0,436
11	196,0	0,783	154,2	11,84	373,76	23,36	0,502
12	216,0	0,756	168,2	11,86	382,41	20,84	0,546
13	235,0	0,819	182,3	11,85	417,14	21,71	0,588
14	254,0	0,827	197,2	11,84	434,58	20,66	0,632
15	271,0	0,835	211,3	11,84	450,35	19,81	0,673
16	287,0	0,842	225,1	11,87	464,70	19,04	0,713
17	302,0	0,848	238,6	11,87	477,77	18,35	0,750
18	316,0	0,854	251,7	11,89	489,97	17,75	0,786
19	330,0	0,860	265,2	11,90	501,93	17,18	0,823
20	344,0	0,865	279,2	11,92	513,37	16,61	0,861
21	356,0	0,870	291,5	11,94	523,25	16,17	0,893
22	369,0	0,874	305,3	11,94	533,34	15,67	0,929
23	380,0	0,879	317,2	11,95	542,27	15,31	0,960
24	391,0	0,883	329,4	11,96	550,73	14,94	0,991
25	402,0	0,887	341,9	11,99	559,08	14,58	1,023
26	412,0	0,890	353,4	12,00	566,29	14,26	1,052
27	422,0	0,894	365,2	12,01	573,77	13,97	1,081
28	430,0	0,897	374,8	12,03	579,62	13,74	1,105
29	440,0	0,901	386,9	12,04	586,86	13,46	1,135
30	449,0	0,904	398,1	12,04	593,14	13,21	1,162
31	458,0	0,907	409,4	12,04	599,30	12,97	1,190
32	466,0	0,910	419,5	12,04	604,78	12,77	1,214
33	474,0	0,913	429,8	12,05	610,21	12,57	1,239
34	481,0	0,916	438,9	12,06	615,02	12,41	1,261
35	489,0	0,918	449,5	12,06	620,02	12,20	1,286
36	496,0	0,921	458,8	12,07	624,71	12,05	1,308
37	503,0	0,923	468,2	12,07	629,0	11,88	1,330
38	509,0	0,926	476,3	12,09	633,1	11,76	1,349
39	516,0	0,928	485,9	12,10	637,3	11,60	1,371
40	522,0	0,931	494,2	12,10	641,3	11,49	1,390
41	528,0	0,933	502,5	12,11	644,9	11,36	1,410
42	534,0	0,935	510,9	12,13	648,5	11,24	1,429
43	540,0	0,937	519,4	12,13	652,0	11,12	1,449
44	545,0	0,939	526,5	12,14	655,0	11,02	1,465
45	550,0	0,941	533,6	12,14	658,0	10,93	1,481
46	556,0	0,943	542,2	12,12	661,5	10,81	1,501
47	561,0	0,945	549,4	12,12	664,4	10,73	1,517
48	566,0	0,947	556,7	12,12	667,3	10,64	1,533

Номер фракции	Температура кипения*, °C	Относительная плотность	Молекулярная масса	Коэффициент Ватсона	Методика (Ющенко, Брусиловский, 2022)		
	Среднее значение				Критическая температура, °C	Критическое давление, бар	Ацентрический фактор
47	561,0	0,945	549,4	12,12	664,4	10,73	1,517
48	566,0	0,947	556,7	12,12	667,3	10,64	1,533
49	570,0	0,949	562,5	12,11	669,7	10,57	1,546
50	575,0	0,951	569,8	12,11	672,6	10,49	1,563
51	579,0	0,953	575,7	12,10	674,9	10,43	1,576
52	584,0	0,955	583,1	12,10	677,7	10,34	1,593
53	588,0	0,956	589,0	12,11	679,8	10,27	1,606
54	592,0	0,958	595,0	12,10	682,1	10,21	1,619
55	596,0	0,960	600,9	12,09	684,4	10,15	1,632
56	600,0	0,961	606,9	12,10	686,4	10,08	1,646
57	604,0	0,963	612,9	12,09	688,7	10,03	1,659
58	608,0	0,965	619,0	12,09	690,9	9,97	1,673
59	612,0	0,966	625,0	12,09	692,9	9,90	1,686
60	615,0	0,968	629,6	12,08	694,7	9,87	1,696
61	619,0	0,969	635,7	12,09	696,6	9,80	1,709
62	622,0	0,971	640,2	12,07	698,4	9,77	1,719
63	625,0	0,972	644,8	12,07	699,9	9,72	1,729
64	629,0	0,974	651,0	12,07	702,0	9,67	1,743
65	632,0	0,975	655,6	12,07	703,5	9,62	1,753
66	635,0	0,976	660,2	12,07	704,9	9,58	1,763
67	638,0	0,978	664,8	12,06	706,7	9,55	1,773
68	641,0	0,979	669,5	12,06	708,1	9,50	1,783
69	644,0	0,981	674,1	12,05	709,8	9,47	1,793
70	647,0	0,982	678,8	12,05	711,3	9,43	1,803
71	650,0	0,983	683,4	12,05	712,7	9,39	1,813
72	653,0	0,984	688,1	12,05	714,1	9,34	1,823
73	655,0	0,986	691,2	12,03	715,4	9,33	1,830
74	658,0	0,987	695,9	12,04	716,8	9,29	1,840
75	661,0	0,988	700,6	12,04	718,1	9,25	1,850
76	664,0	0,989	705,3	12,04	719,5	9,21	1,861
77	667,0	0,991	710,0	12,03	721,2	9,18	1,871
78	670,0	0,992	714,7	12,03	722,5	9,14	1,881
79	673,0	0,993	719,4	12,03	723,8	9,10	1,891
80	675,0	0,994	722,6	12,02	724,8	9,08	1,898